ANTIOXIDANTS & REDOX SIGNALING
Volume 15, Number 11, 2011

DOI: 10.1089/ars.2010.3713

ORIGINAL RESEARCH COMMUNICATION

Lipopolysaccharide-Induced Mitochondrial DNA Depletion

Amal Choumar,[1,2] Arige Tarhuni,[1,2] Philippe Lettéron,[1,2] Florence Reyl-Desmars,[1,2] Nismah Dauhoo,[1,2] Julie Damasse,[1,2] Nathalie Vadrot,[1,2] Pierre Nahon,[1,2] Richard Moreau,[1,2] Dominique Pessayre,[1,2] and Abdellah Mansouri[1,2]

Abstract

Hepatic energy depletion has been described in severe sepsis, and lipopolysaccharide (LPS) has been shown to cause mitochondrial DNA (mtDNA) damage. To clarify the mechanisms of LPS-induced mtDNA damage and mitochondrial alterations, we treated wild-type (WT) or transgenic manganese superoxide dismutase-overexpressing ($MnSOD^{+++}$) mice with a single dose of LPS (5 mg/kg). In WT mice, LPS increased mitochondrial reactive oxygen species formation, hepatic inducible nitric oxide synthase (NOS) mRNA and protein, tumor necrosis factor-alpha, interleukin-1 beta, and high-mobility group protein B1 concentrations. Six to 48 h after LPS administration (5 mg/kg), liver mtDNA levels, respiratory complex I activity, and adenosine triphosphate (ATP) contents were decreased. In addition, LPS increased interferon-β concentration and decreased mitochondrial transcription factor A (Tfam) mRNA, Tfam protein, and mtDNA-encoded mRNAs. Morphological studies showed mild hepatic inflammation. The LPS (5 mg/kg)-induced mtDNA depletion, complex I inactivation, ATP depletion, and alanine aminotransferase increase were prevented in $MnSOD^{+++}$ mice or in WT mice cotreated with 1400W (a NOS inhibitor), (2-(2,2,6,6-tetramethylpiperidin-1-oxyl-4-ylamino)-2-oxoethyl)triphenylphosphonium chloride, monohydrate (a superoxide scavenger) or uric acid (a peroxynitrite scavenger). The MnSOD overexpression delayed death in mice challenged by a higher, lethal dose of LPS (25 mg/kg). In conclusion, LPS administration damages mtDNA and alters mitochondrial function. The protective effects of MnSOD, NOS inhibitors, and superoxide or peroxynitrite scavengers point out a role of the superoxide anion reacting with NO to form mtDNA- and protein-damaging peroxynitrite. In addition to the acute damage caused by reactive species, decreased levels of mitochondrial transcripts contribute to mitochondrial dysfunction. *Antioxid. Redox Signal.* 15, 2837–2854.

Introduction

Life-threatening effects of sepsis (39) involve an excessive formation of inflammatory cytokines, reactive oxygen species (ROS), and reactive nitrogen species (RNS) (26), thereby leading to oxidative stress, mitochondrial dysfunction, and organ failure (44).

Septic shock can be triggered by lipopolysaccharide (LPS), which stimulates the production of tumor necrosis factor-alpha (TNF-α) and other cytokines in macrophages and immune cells, leading to ROS generation (17). The NADPH oxidases (NOX) of hepatic macrophages liberate ROS partly in the extracellular space, the mitochondria of hepatocytes generate ROS inside the cells. In many cell types, TNF-α-induced ROS production occurs mainly within the mitochondria (13). Interferon-γ (IFN-γ) also increases mitochondrial ROS production in hepatocytes (46).

Although mitochondria form large amounts of the superoxide radical anion (henceforward referred to as superoxide), mitochondrial manganese superoxide dismutase (MnSOD) accelerates its dismutation into hydrogen peroxide, which is detoxified into water by mitochondrial glutathione peroxidase, mitochondrial peroxiredoxins, and peroxisomal catalase (45). The MnSOD is inducible by ROS, cytokines, alcohol, and LPS (7, 18), but it is inactivated by peroxynitrite (8, 27). The MnSOD decreases superoxide concentrations (25), thus limiting the formation of peroxynitrite, a strong oxidant generated by the reaction of superoxide with nitric oxide (9, 37). Peroxynitrite and peroxynitrite-generated reactive intermediates can nitrate proteins and damage lipids and DNA (1, 9, 34, 37), and they may be involved in mitochondrial DNA (mtDNA) depletion after acetaminophen or alcohol administration (5, 19). In keeping with the role of inducible nitric oxide synthase (iNOS) in LPS-induced liver lesions (6, 29) and the ability of MnSOD to decrease peroxynitrite formation, a recombinant adenovirus increasing MnSOD protected against LPS-induced mitochondrial oxidative stress in cardiomyocytes (50).

The mtDNA is more susceptible to oxidative damage than nuclear DNA (nDNA), due to incomplete DNA repair

[1]INSERM, U773, Centre de Recherche Biomédicale Bichat Beaujon CRB3, Paris, France.
[2]Université Paris Diderot, Sorbonne Paris Cité, Paris, France.

capacity in mitochondria and the proximity of mtDNA to the respiratory chain, an important source of ROS (48). The ROS and RNS can oxidatively damage mitochondrial proteins, phospholipids, and mtDNA (19, 47), thus causing the formation of 8-hydroxydeoxyguanosine (47), apurinic/apyrimidinic sites, and strand breaks in mtDNA (32) and occasionally triggering mtDNA deletions (31). Extensive mtDNA lesions cause nuclease-mediated mtDNA degradation, thereby leading to mtDNA depletion (19, 32), which can impair the synthesis of the 13 mtDNA-encoded proteins of respiratory chain complexes I, III, IV, and V (4).

The mtDNA replication and transcription are modulated by nuclear factors and coactivators. Peroxisome proliferator-activated receptor gamma coactivator 1 (PGC-1) interacts with nuclear respiratory factors 1 and 2 (NRF-1 and NRF-2) to transactivate several oxidative phosphorylation system (OXPHOS) genes (3, 22, 24). In fact, PGC-1, NRF-1, and NRF-2 also mediate mtDNA transcription and replication by inducing mitochondrial transcription factor B and mitochondrial transcription factor A (Tfam) (33, 38). The Tfam initiates transcription (and transcription-initiated replication) (16, 38). The Tfam knockout mice have low mtDNA levels; they lack OXPHOS and die during embryogenesis (20). Interestingly, IFN-α and IFN-γ suppress mitochondrial gene transcription by depleting Tfam mRNA and protein (14). Type I IFNs also activate mitochondrial RNase L, which degrades mtDNA-encoded mRNAs (23). Since LPS administration induces IFN-γ and type I IFNs (35), it could also have some of these effects.

The administration of LPS or inactivated crude *Escherichia coli* bacteria to mice increased mitochondrial ROS and decreased cardiac and hepatic mtDNA levels (40–42). These effects of LPS on mtDNA did not occur in Toll-like receptor 4 (TLR4)-deficient mice, thus indicating the role of TLR4 signaling (42). However, downstream mechanisms causing mtDNA depletion were not delineated.

The goal of the present study was to dissect the mechanisms of mtDNA depletion and mitochondrial dysfunction after LPS administration to mice. We selected a dose of LPS (5 mg/kg) that decreased mtDNA levels and mitochondrial function without causing severe liver lesions. The LPS-induced mtDNA depletion and mitochondrial dysfunction were prevented or attenuated in transgenic MnSOD-overexpressing ($MnSOD^{+++}$) mice, or when wild-type (WT) mice were treated with substances aimed at scavenging peroxynitrite or decreasing the reaction of mitochondrial superoxide with NO to form peroxynitrite. These data provide new insight into the molecular mechanisms underlying a major clinical problem, namely the frequent occurrence of severe multiorgan failure, despite sometimes modest tissue lesions in patients with severe sepsis. Our observation that LPS-induced mitochondrial dysfunction is preventable in mice raises the hope that the dire prognosis of severe sepsis could be therapeutically improved in humans.

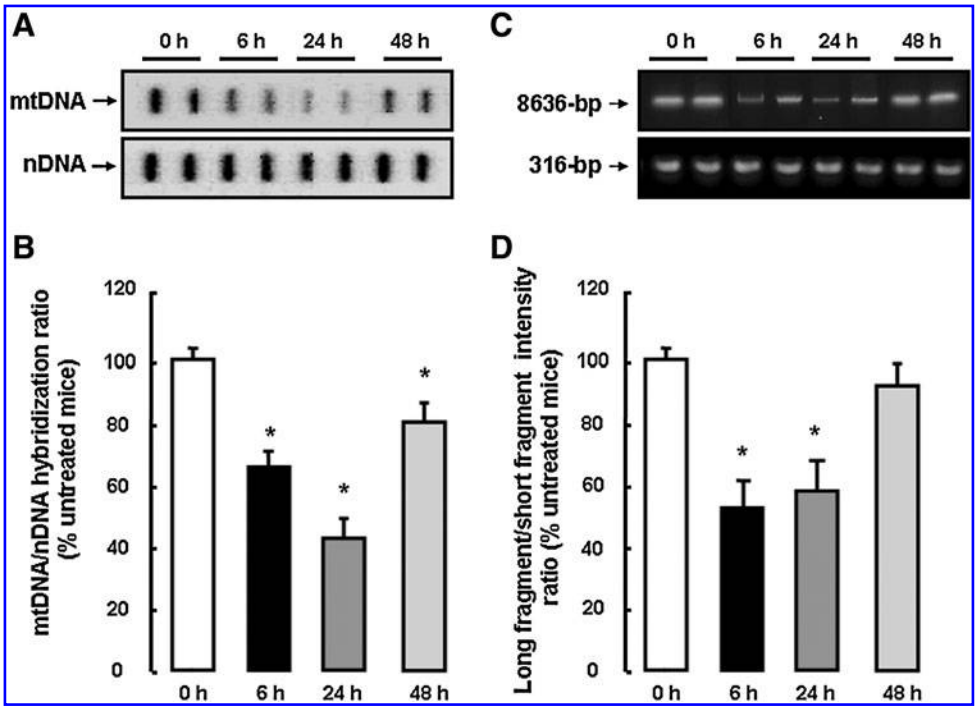

FIG. 1. Effects of lipopolysaccharide (LPS) administration on mitochondrial DNA (mtDNA) levels and integrity. Wild-type (WT) mice that were killed 6, 24, or 48 h after the administration of water served as pooled zero-time controls (0 h) for mice sacrificed 6, 24, or 48 h after LPS (5 mg/kg) administration. **(A)** Total hepatic DNA (300 ng) was blotted onto a nylon membrane, hybridized with a 10.9-kb mtDNA probe, stripped, and rehybridized with a mouse C_ot-1 nuclear DNA (nDNA) probe. **(B)** For each mouse, blot intensities were determined by densitometry analysis, and the mtDNA/nDNA hybridization ratio was calculated and expressed as the percentage of the mean value for untreated mice. Values represent means ± standard error of the mean (SEM) for 15 mice. *Different from untreated mice (0 h), $p < 0.05$. **(C)** Long polymerase chain reaction (PCR) was used to assess the presence of mtDNA lesions hampering the progress of DNA polymerases. Total hepatic DNA was prepared, and used to amplify both a long (8636-bp) mtDNA fragment and a short (316-bp) mtDNA fragment as shown in the representative photograph. **(D)** Lesions hampering replication are much more likely to be present on a long DNA fragment than on a short DNA fragment. For each mouse, the long fragment/short fragment hybridization ratio was quantified and expressed as the percentage of the mean value in untreated mice. Results are expressed as mean ± SEM in five to eight mice. *Different from untreated mice (0 h), $p < 0.05$.

Results

LPS administration decreased mtDNA levels, mtDNA integrity, complex I activity, and hepatic adenosine triphosphate

The LPS administration decreased hepatic mtDNA levels assessed by slot-blot hybridization without affecting nDNA content (Fig. 1A). We, thus, used the mtDNA/nDNA hybridization ratio to assess LPS-induced mtDNA changes (Fig. 1B). This ratio was decreased by 33%, 57%, and 19%, 6, 24, and 48 h, respectively after LPS administration (Fig. 1B). We also used quantitative real-time polymerase chain reaction (qRT-PCR) with primers specific for subunit 2 of cytochrome *c* oxidase (COX2) to confirm LPS-induced mtDNA depletion (Supplementary Fig. S1; Supplementary Data are available online at www.liebertonline.com/ars). To assess the presence of mtDNA lesions blocking the progress of polymerases, we performed long PCR experiments to concomitantly amplify a long (8636-bp) and a short (316-bp) mtDNA fragment (Fig. 1C). The DNA lesions blocking replication are more likely to be present on a long DNA region than on a short fragment (32). Indeed, the amplification of the short DNA fragment was similar in all groups of mice (Fig. 1C). We, therefore, used the long fragment/short fragment intensity ratio as an index of mtDNA integrity (Fig. 1D). This ratio was significantly decreased by 47% 6 h and by 40% 24 h after LPS administration, but was again normal in 48 h after LPS administration (Fig. 1D).

Complex I activity was decreased by 43%, 57%, and 45%, and hepatic adenosine triphosphate (ATP) by 33%, 41%, and 24% in 6, 24, and 48 h, respectively, after LPS administration (Fig. 2).

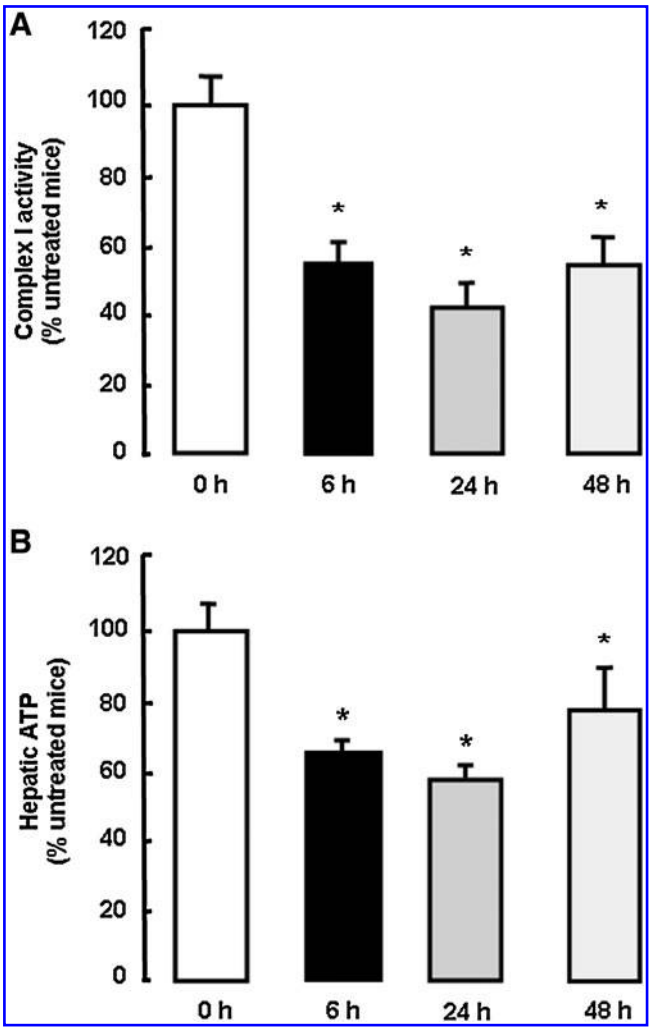

FIG. 2. Effects of LPS administration on complex I activity and hepatic adenosine triphosphate (ATP) levels. The WT mice which were killed 6, 24, or 48 h after the administration of water served as pooled zero-time controls (0 h) for mice sacrificed 6, 24, or 48 h after LPS administration (5 mg/kg). **(A)** Hepatic mitochondria were isolated, and submitochondrial particles were prepared. Complex I was assayed by following the oxidation of NADH in the presence of decylubiquinone and antimycin A. Results are expressed as mean ± SEM in 15 mice. *Different from untreated mice (0 h), $p < 0.05$. **(B)** The liver was quickly excised and ground in liquid nitrogen. Hepatic ATP was measured with a luciferin/luciferase assay. Results are expressed as mean ± SEM in 10 mice. *Different from untreated mice (0 h), $p < 0.05$.

The LPS-induced increase in mitochondrial ROS and thiobarbituric acid reactants was attenuated by (2-(2,2,6,6-tetramethylpiperidin-1-oxyl-4-ylamino)-2-oxoethyl)triphenylphosphonium chloride, monohydrate administration

One mechanism that could damage and deplete mtDNA after LPS administration could be ROS-mediated mtDNA damage. The LPS administration increased mitochondrial thiobarbituric acid reactants (TBARs), an index of lipid peroxidation, and led to decreased aconitase activity (Table 1), an index of oxidative stress (36). The *in vitro* formations of superoxide and peroxides (assessed with the MitoSOX™ Red reagent and 2′,7′-dichlorodihydrofluorescein diacetate [H_2DCF-DA], respectively) were decreased in liver mitochondria isolated after LPS administration and energized with malate and glutamate (two complex I substrates) or succinate (a complex II substrate) (Table 1). The LPS administration also decreased the peroxynitrite- and peroxide-driven oxidation of dihydrorhodamine 123 (DHR123) into rhodamine 123 by a whole-liver homogenate incubated with succinate or malate and glutamate (Table 1). Plasma nitrite/nitrate concentrations were still unchanged 6 h after LPS, but increased by 48% and 67% in 24 and 48 h, respectively, after LPS administration (Table 1). Plasma or hepatic iron contents were similar in control and LPS-treated mice (Table 1).

(2-(2,2,6,6-Tetramethylpiperidin-1-oxyl-4-ylamino)-2-oxoethyl)triphenylphosphonium chloride, monohydrate (Mito-TEMPO) administration totally or partially prevented the LPS-induced inhibition of aconitase, increase in mitochondrial ROS formation, and increase in TBARs without preventing the LPS-induced increase in plasma nitrite/nitrate concentration (Table 1).

Although apocynin did not prevent mtDNA depletion, Mito-TEMPO, nitro-L-arginine methyl ester, 1400W, or uric acid protected against LPS-induced mtDNA depletion and complex I impairment

To gain further insight into the type and origin of the reactive species involved in mtDNA depletion, we treated WT mice with diverse substances (Table 2). None of these treatments given alone (without LPS) modified mtDNA levels.

Table 1. Effect of Lipopolysaccharide With or Without (2-(2,2,6,6-Tetramethylpiperidin-1-Oxyl-4-Ylamino)-2-Oxoethyl)Triphenylphosphonium Chloride, Monohydrate Administration on Aconitase Activity, Mitochondrial Reactive Oxygen Species Formation, Mitochondrial Thiobarbituric Acid Reactants, Plasma Nitrite/Nitrate Levels, Plasma Iron, and Liver Iron

	LPS				*LPS + Mito-TEMPO*
	0 h	*6 h*	*24 h*	*48 h*	*24 h*
Aconitase (nmol/min/mg protein)	0.76 ± 0.10	0.38 ± 0.09[a]	0.41 ± 0.08[a]	0.52 ± 0.11[a]	0.59 ± 0.11[b]
ROS formation (% control mice)					
Mitochondria + MitoSOX + mal/glu	100 ± 11	160 ± 13[a]	144 ± 15[a]	142 ± 8[a]	108 ± 8[b]
Mitochondria + MitoSOX + succinate	100 ± 9	181 ± 18[a]	162 ± 12[a]	178 ± 25[a]	122 ± 15[b]
Mitochondria + H_2DCF + mal/glu	100 ± 8	141 ± 10[a]	145 ± 11[a]	134 ± 13[a]	121 ± 9[b]
Mitochondria + H_2DCF + succinate	100 ± 14	208 ± 29[a]	200 ± 18[a]	188 ± 22[a]	144 ± 12[ab]
Homogenate + DHR123 + mal/glu	100 ± 16	136 ± 14[a]	166 ± 11[a]	114 ± 7	128 ± 12[b]
Homogenate + DHR123 + succinate	100 ± 21	138 ± 12[a]	191 ± 27[a]	119 ± 18	136 ± 9[ab]
Mitochondrial TBARs (nmol/mg protein)	0.34 ± 0.04	0.52 ± 0.10[a]	0.59 ± 0.12[a]	0.44 ± 0.08	0.40 ± 0.06[b]
Plasma nitrite/nitrate (μM)	46 ± 4	43 ± 9	68 ± 12[a]	77 ± 11[a]	71 ± 9[a]
Plasma iron (μM)	20 ± 4	18 ± 4	23 ± 5	ND	ND
Hepatic iron (μmol/kg)	97 ± 11	122 ± 14	114 ± 14	ND	ND

Mice killed at 6, 24, or 48 h after the administration of water served as pooled zero-time controls (0 h) for mice sacrificed after LPS (5 mg/kg) administration. Some mice received Mito-TEMPO (50 mg/kg body weight i.p.), a mitochondria-targeted superoxide scavenger, 30 min before and 8 h after LPS administration. Mitochondrial ROS formation was evaluated by recording the relative fluorescence of specific fluorogenic dyes. Mitochondrial superoxide formation was detected with MitoSOX Red, and mitochondrial peroxide formation with H_2DCF after incubation of mitochondria with either mal/glu or succinate. The formation of peroxynitrite and other ROS in a whole-liver homogenate was evaluated with the mitochondrial-avid dye, DHR123. Values are expressed as mean ± SEM for 10–15 mice.

[a]Different from control mice (0 h) ($p < 0.05$, one-way ANOVA).

[b]Different from LPS-treated mice not treated with Mito-TEMPO.

LPS, lipopolysaccharide; SEM, standard error of the mean; Mito-TEMPO, (2-(2,2,6,6-tetramethylpiperidin-1-oxyl-4-ylamino)-2-oxoethyl)-triphenylphosphonium chloride, monohydrate; H_2DCF-DA, 2′,7″-dichlorodihydrofluorescein diacetate; ND, not determined; mal/glu, malate/glutamate; DHR123, dihydrorhodamine 123; TBARs, thiobarbituric acid reactants; ROS, reactive oxygen species; i.p., intraperitoneally; ANOVA, analysis of variance.

Although apocynin significantly inhibited NOX (Supplementary Fig. S2), it did not prevent mtDNA depletion in LPS-treated mice (Table 2). In contrast, Mito-TEMPO (a mitochondria-targeted superoxide scavenger), nitro-L-arginine methyl ester (L-NAME) (a broad spectrum NOS inhibitor), 1400W (a specific inhibitor of iNOS), or uric acid (a peroxynitrite scavenger) partially or totally protected against LPS-induced mtDNA depletion and complex I impairment (Table 2). These effects suggested that peroxynitrite, generated from a reaction between superoxide anion and NO, played a role in this process. These results also indicated that the superoxide involved in this reaction was mainly produced by mitochondria rather than by NOX.

LPS administration increased iNOS expression but decreased MnSOD protein, despite the induction of the MnSOD mRNA after LPS administration

The expression of the iNOS mRNA increased 16-fold 6 h after LPS administration, but had returned to control values at 24 or 48 h (Fig. 3A). The iNOS protein increased 4.5-fold at 6 h and 5-fold at 24 h after LPS administration (Fig. 3B). Despite an increase in MnSOD mRNA (Fig. 3C), MnSOD protein decreased 6 and 24 h after LPS administration to WT mice, with a parallel decline in MnSOD activity (Fig. 4A, B).

Mito-TEMPO or uric acid administration, but not MnSOD overexpression, prevented the decrease in MnSOD protein after LPS administration

Mito-TEMPO or uric acid administration to WT mice prevented the LPS-mediated decrease in MnSOD protein and activity (Fig. 4). In contrast, MnSOD overexpression did not prevent the fall in $MnSOD^{+++}$ protein and activity after LPS administration (Fig. 4). However, due to its threefold higher initial value, MnSOD protein remained higher after LPS administration in $MnSOD^{+++}$ mice than in WT mice (Fig. 4A). Similar data were obtained when MnSOD activity and protein levels were evaluated in the mitochondrial fractions and normalized to mg of mitochondrial proteins as well as to mg of wet tissue. Unlike that of MnSOD, the activity of copper-zinc superoxide dismutase (Cu,ZnSOD) was similar in untreated or LPS-treated WT and $MnSOD^{+++}$ mice (Supplementary Fig. S3).

MnSOD overexpression, or the administration of Mito-TEMPO, uric acid, or 1400W to WT mice, prevented or attenuated the LPS-induced nitration of tyrosine residues in mitochondrial respiratory chain complex proteins

There were no changes in the protein levels of mitochondrial respiratory chain complexes separated by blue native polyacrylamide gel electrophoresis 6 or 24 h after LPS administration (Fig. 5A). Proteins were transferred onto nitrocellulose membranes and revealed with an antibody against 3-nitrotyrosine (Fig. 5B). In untreated mice, 3-nitrotyrosine was not detected in the proteins of complexes I and III, but was present in complex V proteins (Fig. 5B). The LPS administration to WT mice, but not to $MnSOD^{+++}$ mice, led to the development of nitrotyrosine residues in the proteins of complexes I and III and increased nitrotyrosine in complex V proteins. The administration of Mito-TEMPO, uric acid, or 1400W to WT mice likewise prevented the

Table 2. Effects of a Superoxide Scavenger [(2-(2,2,6,6-Tetramethylpiperidin-1-Oxyl-4-Ylamino)-2-Oxoethyl)-Triphenylphosphonium Chloride, Monohydrate], Nonselective Nitric Oxide Synthase Inhibitor (Nitro-L-Arginine Methyl Ester), Specific Inducible Nitric Oxide Synthase Inhibitor (1400W), Peroxynitrite Scavenger (Uric Acid), or Reduced Nicotinamide-Adenine Dinucleotide Phosphate Oxidase Inhibitor (Apocynin) on Lipopolysaccharide-Induced Mitochondrial DNA Depletion and Complex I Impairment

	mtDNA/nDNA hybridization ratio (% untreated mice)			*Complex I activity (% untreated mice)*		
Treatment	*0 h*	*6 h*	*24 h*	*0 h*	*6 h*	*24 h*
LPS	100 ± 7	60 ± 5[a]	51 ± 7[a]	100 ± 14	68 ± 10[a]	50 ± 15[a]
LPS + Mito-Tempo	100 ± 8	102 ± 11[b]	92 ± 8[b]	99 ± 12	88 ± 10[b]	83 ± 8[b]
LPS + L-NAME	98 ± 6	88 ± 5[b]	88 ± 4[b]	91 ± 10	91 ± 21[b]	93 ± 2[b]
LPS + 1400W	104 ± 10	89 ± 8[b]	92 ± 10[b]	98 ± 9	88 ± 8[b]	88 ± 10[b]
LPS + uric acid	99 ± 9	91 ± 4[b]	79 ± 11[ab]	111 ± 14	82 ± 3[b]	74 ± 8[ab]
LPS + apocynin	102 ± 10	74 ± 6[a]	60 ± 10[a]	ND	ND	ND

Mice killed 6 or 24 h after the administration of water served as pooled zero-time controls (0 h) for mice sacrificed after LPS (5 mg/kg) administration. Thirty minutes before LPS, some mice received an intraperitoneal injection of Mito-TEMPO (50 mg/kg body weight), L-NAME (80 mg/kg body weight), 1400W (10 mg/kg body weight), uric acid (500 mg/kg body weight), or apocynin (20 mg/kg body weight). A second dose of the cotreatment was administered 8 h after LPS administration in mice that were to be sacrificed 24 h after LPS injection. Values represent means ± SEM for 6–10 mice.

[a]Different from untreated mice (0 h) receiving the same cotreatment, if any ($p < 0.05$, one-way ANOVA).

[b]Different from mice treated with LPS alone and studied at the same treatment time ($p < 0.05$, one-way ANOVA).

L-NAME, nitro-L-arginine methyl ester; mtDNA, mitochondrial DNA; nDNA, nuclear DNA.

development of nitrotyrosine residues in complex III after LPS administration and attenuated their increased formation in complexes I and V proteins (Fig. 5B).

MnSOD overexpression protected against LPS-induced mtDNA depletion and complex I impairment

Unlike its effects in WT mice, LPS administration did not decrease mtDNA levels in MnSOD^{+++} mice (Fig. 6A, B). The MnSOD overexpression also prevented the LPS-mediated decrease in complex I activity 6 h after LPS administration and attenuated it at 24 h (Fig. 6C). These results suggested that the superoxide anion, in particular that produced within the mitochondria, played a direct or indirect role in triggering LPS-induced mtDNA depletion and complex I impairment.

MnSOD overexpression prevented the LPS-induced increase in plasma interleukin-1β and high mobility group protein B1 levels but not the increase in TNF-α

The LPS significantly increased interleukin-1β (IL-1β) and high mobility group protein B1 (HMGB1) levels in WT mice but not in MnSOD^{+++} mice (Supplementary Fig. S4). However, LPS similarly increased TNF-α levels in either WT or MnSOD^{+++} mice (Fig. 7A).

Pentoxifylline prevented the LPS-mediated increase in TNF-α without preventing mtDNA depletion in WT mice

Pentoxifylline prevented the LPS-mediated TNF-α surge without preventing mtDNA depletion (Fig. 7B, C), suggesting that several redundant mechanisms other than TNF-α may be involved in ROS formation and mtDNA depletion after LPS administration.

LPS decreased the levels of Tfam transcripts and protein, but not the PGC-1 protein level

Another mechanism that could play a role in impaired mitochondrial function could be a decreased expression of factors that modulate mtDNA replication and/or transcription. Although the PGC-1 protein was not affected by the LPS treatment, the Tfam mRNA was decreased by 53% and 47%, and the Tfam protein by 41% and 51% 6 and 24 h, respectively after LPS administration (Fig. 8). Both the Tfam mRNA and the Tfam protein had returned to control values by 48 h (Fig. 8).

LPS increased IFN-β and caused a decrease in mitochondrial mRNAs that was partially prevented by chloramphenicol

Although its mean value was already high at that time, IFN-β was not yet significantly increased 6 h after LPS administration, but was significantly increased fourfold 24 h after LPS administration (Fig. 9A). Type I IFNs can suppress mitochondrial gene transcription by depleting Tfam mRNA (14) and by activating RNase L, which is also expressed within mitochondria and can degrade mtDNA-encoded mRNAs in a translation-dependent process that is inhibited by chloramphenicol (23). Although chloramphenicol had no protective effect on the LPS-induced increase in plasma IFN-β (Fig. 9A) nor on LPS-induced mtDNA depletion (Fig. 9B), it partially prevented the decreases in COX2 and NADH-dehydrogenase subunit 1 (ND1) mRNAs at 24 h, but not at 6 h, after LPS administration (Fig. 9C, D).

The LPS treatment triggered mild hepatic inflammation, but neither necrosis nor apoptosis

Liver histology was evaluated in control mice and mice treated with LPS for 6, 24, or 48 h. No inflammation, steatosis, necrosis, or apoptosis were observed in 10 control mice or 10 mice treated with LPS for 6 or 24 h. However, four of the 10 mice treated for 48 h ($\chi^2 = 13.33$; $p < 0.05$) exhibited moderate inflammation without necrosis or apoptosis (Supplementary Fig. S5). Hepatic caspase-3 activity was similar in control mice and mice sacrificed 6 or 24 h after LPS administration (51 ± 10, 53 ± 7, and 55 ± 9 pmol/min/mg protein, respectively). Even with the sensitive C_ot-1 hybridization technique, we could not detect nDNA fragmentation in any of these mice.

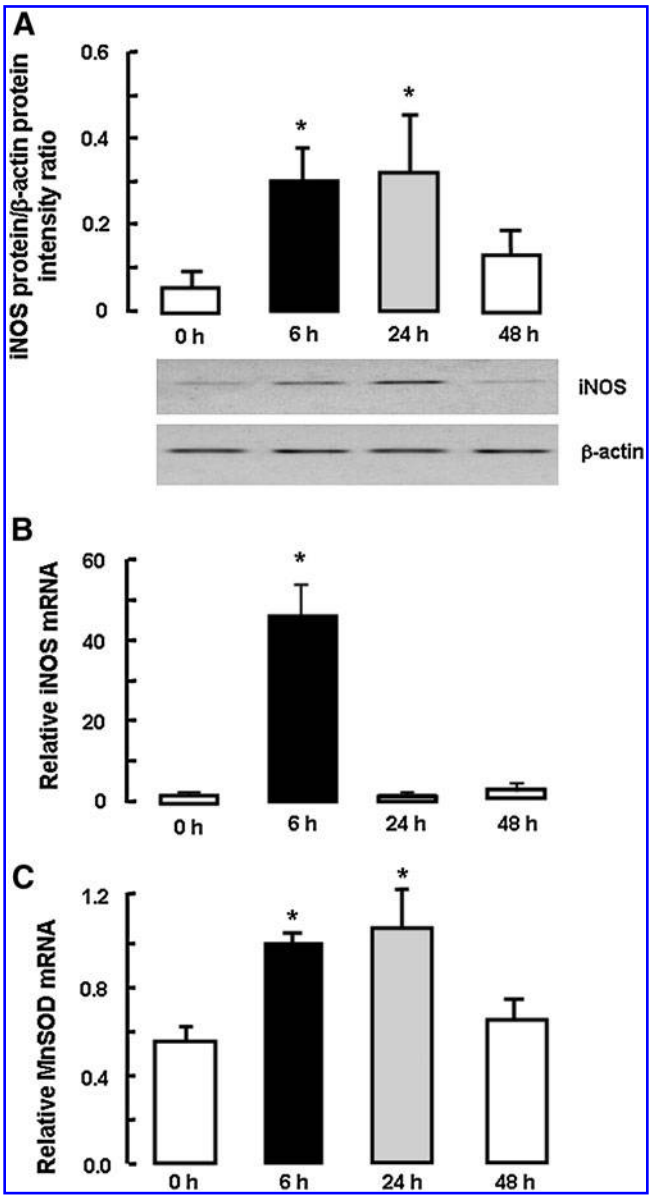

FIG. 3. Effects of LPS on inducible nitric oxide synthase (iNOS) protein and mRNA and manganese superoxide dismutase (MnSOD) mRNA. The WT mice killed 6, 24, or 48 h after the administration of water served as pooled zero-time controls (0 h) for mice sacrificed 6, 24, or 48 after LPS administration (5 mg/kg). **(A)** Representative immunoblot of the iNOS protein and its quantification. **(B, C)** Total hepatic RNA (2 μg) was reverse-transcribed, and cDNA underwent quantitative real-time (qRT)-PCR with primers specific to S6 (ribosomal protein S6) and either iNOS **(B)** or MnSOD **(C)**. The relative iNOS mRNA or MnSOD mRNA expression was normalized to the S6 mRNA. Results are expressed as mean ± SEM for six to eight mice. *Different from untreated mice (0 h) ($p < 0.05$, one-way analysis of variance [ANOVA]).

MnSOD overexpression or the administration of Mito-TEMPO, uric acid, or 1400W to WT mice prevented alanine aminotransferase elevation and hepatic ATP depletion after LPS administration; and MnSOD overexpression delayed death after a higher dose of LPS

Plasma alanine aminotransferase (ALT) activity was unchanged in mice killed at 6 or 24 h after LPS administration but was significantly increased by 68% at 48 h after LPS (Fig. 10A). The MnSOD overexpression or the administration of Mito-TEMPO, uric acid, or 1400W to WT mice prevented the decrease in hepatic ATP at 24 h after LPS administration (Fig. 10B) and the increase in plasma ALT activity at 48 h after LPS administration (Fig. 10A).

Although the 5 mg/kg-dose used in all previous experiments exceptionally caused death (Fig. 11A), a higher LPS dose (25 mg/kg) markedly decreased survival (Fig. 11B). The MnSOD overexpression delayed death after this high dose of LPS (Fig. 11B).

LPS increased TLR-4 protein expression and mitochondrial superoxide formation and depleted mtDNA in HepG2 hepatoma cells

To assess whether hepatocytes themselves can respond to LPS by increasing ROS formation, HepG2 hepatoma cells were treated with LPS (5 μg/ml) for 6 or 24 h with or without Mito-TEMPO (Fig. 12). The LPS increased TLR-4 protein expression (Fig. 12A) and mitochondrial superoxide formation (Fig. 12B) and depleted mtDNA (Fig. 12C). The Mito-TEMPO fully prevented these LPS-induced effects (Fig. 12B, C).

IFN-β decreased the mtDNA-encoded COX2 mRNA in HUH7 human hepatoma cells

To confirm that type I IFNs can decrease mitochondrial transcripts, IFN-responsive HUH7 cells were treated with IFN-β (1000 U/ml) for 2, 6, or 24 h (Supplementary Fig. S6). The IFN-β halved COX2 mRNA as soon as 2 h after its addition (Supplementary Fig. S6D), even though IFN-β had no significant effects on mitochondrial superoxide formation (Supplementary Fig. S6A), the concentration of nitrite/nitrate in the culture medium (Supplementary Fig. S6B), or mtDNA levels, which were normal at 2 or 6 h, although they later slightly decreased at 24 h (Supplementary Fig. S6C).

Discussion

Our objectives were to assess the mechanisms for mtDNA damage after LPS administration and look for protective strategies that could prevent these adverse effects. We found that hepatic mtDNA was severely damaged and depleted (Fig. 1), and mitochondrial function markedly impaired 6–48 h after LPS administration to WT mice (Fig. 2). We also showed for the first time that LPS-induced mtDNA depletion and mitochondrial dysfunction could be prevented by various strategies aimed at scavenging peroxynitrite or decreasing the reaction of mitochondrial superoxide with NO to form peroxynitrite (Table 2 and Fig. 6).

From previous data and present findings, we propose that LPS triggers the successive events suggested in Figure 13. The interaction of LPS with TLR4 on Kupffer cells activates NOXs

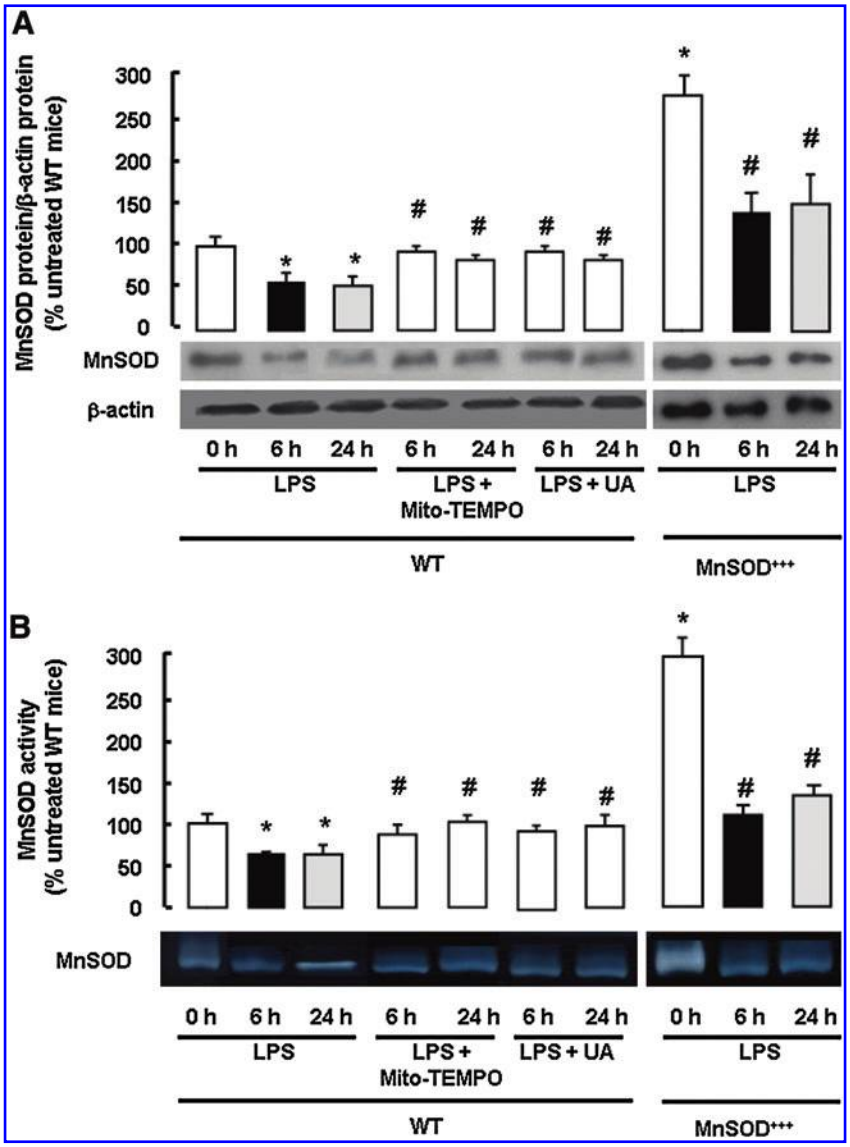

FIG. 4. Effects of LPS on MnSOD protein and MnSOD activity. WT and transgenic MnSOD-overexpressing ($MnSOD^{+++}$) mice killed 6, 24, or 48 h after the administration of water served as pooled zero-time controls (0 h) for mice sacrificed 6, 24, or 48 h after LPS (5 mg/kg) administration. Some WT mice were treated with (2-(2,2,6,6-tetramethylpiperidin-1-oxyl-4-ylamino)-2-oxoethyl)-triphenylphosphonium chloride, monohydrate (Mito-TEMPO) (50 mg/kg) or uric acid (UA) (500 mg/kg) 30 min before and 8 h after LPS administration. Hepatic homogenates were prepared, and proteins underwent sodium dodecyl sulfate (SDS)-polyacrylamide gel electrophoresis (PAGE), transfer, and recognition by anti-MnSOD and anti-β-actin antibodies. Other protein samples underwent native gel electrophoresis, and SOD activity was assayed within the gel. **(A)** Representative immunoblots and quantification of the MnSOD protein (mean ± SEM) in 15 mice. **(B)** Representative in-gel activity and quantification of the MnSOD activity (mean ± SEM) in 5–11 mice. *Different from control (0 h), $p < 0.05$. #Different from WT mice studied at the same treatment time (6 or 24 h) ($p < 0.05$, two-way ANOVA). (To see this illustration in color the reader is referred to the web version of this article at www.liebertonline.com/ars).

that release superoxide outside the cell. The LPS also releases TNF-α and IFN-γ, both of which increase the mitochondrial formation of superoxide in hepatocytes (2, 44, 46). Although Mito-TEMPO, a superoxide scavenger, prevented LPS-mediated mtDNA depletion in WT mice, apocynin, albeit effective in inhibiting NOX (Supplementary Fig. S2), did not prevent mtDNA depletion (Table 2). Further, LPS did not deplete mtDNA in transgenic mice overexpressing MnSOD (Fig. 6), whose role is to decrease the mitochondrial concentrations of superoxide. These observations indicate a predominant role of mitochondria-generated superoxide in triggering mtDNA depletion (Fig. 13).

Except for its reactivity with iron-sulfur complexes, the superoxide itself is poorly reactive with biological molecules. However, it reacts with NO to form the highly reactive peroxynitrite (9). The conjunction of an increased mitochondrial superoxide formation (Table 1) with an increased iNOS expression (Fig. 3A, B) (29) should markedly increase the mitochondrial formation of peroxynitrite after LPS administration (Fig. 13). Although the presence of NOS within mitochondria is debated, the freely diffusible NO formed elsewhere can cross mitochondrial membranes to react with superoxide and form peroxynitrite within the mitochondria (37).

Peroxynitrite and/or peroxynitrite-generated reactive intermediates can damage mtDNA (5, 9, 19). In the present study, L-NAME, a broad-spectrum NOS inhibitor (34), 1400W, a selective iNOS inhibitor (34), or uric acid, a peroxynitrite scavenger (12), all prevented or attenuated LPS-induced mtDNA depletion (Table 2). Although the specificity of these various scavengers for a given species may not be perfect, taken together, these observations suggest that the reaction of superoxide with NO to form the DNA-damaging peroxynitrite (9) is involved in the mtDNA damage triggered by LPS (Fig. 13). Six or 24 h after LPS administration, mtDNA was severely depleted (Fig. 1A, B), probably because damaged mtDNA molecules had been degraded by mitochondrial nucleases (19, 32). Further, remaining mtDNA molecules presented mtDNA lesions, as shown by selective impairment of the amplification of a long mtDNA fragment contrasting with normal amplification of a short fragment (Fig. 1C, D). Lesions hampering the progress of polymerases are more likely to be present on a long stretch of DNA than a short DNA region (19, 32).

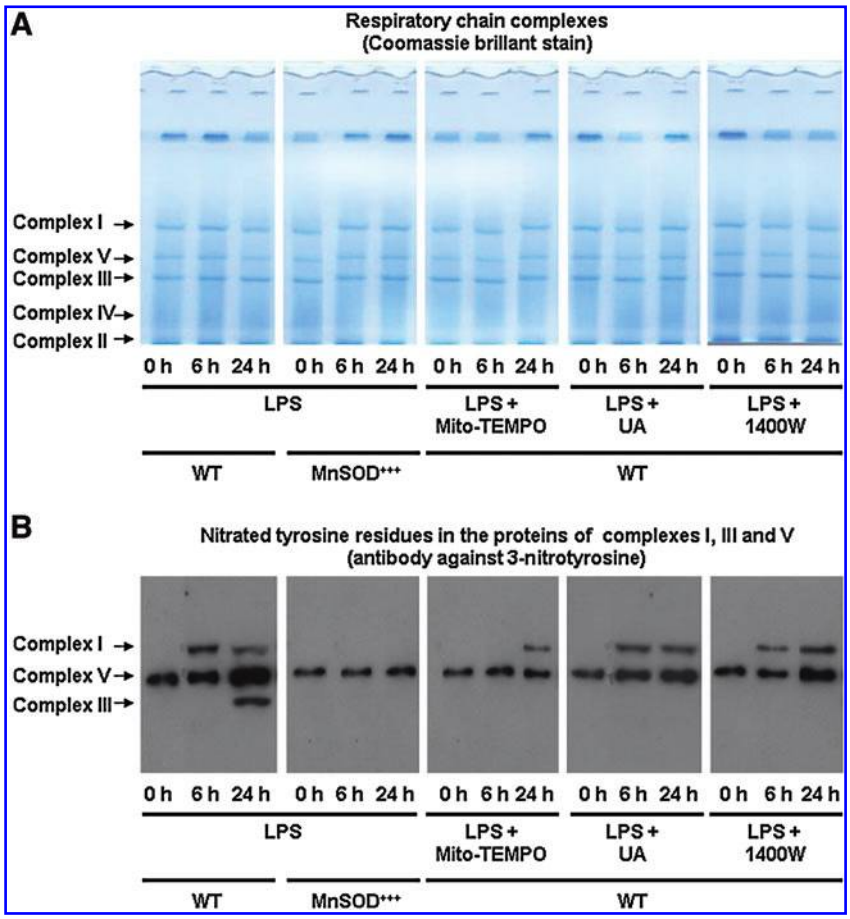

FIG. 5. Effects of LPS administration on the proteins of mitochondrial respiratory chain complexes and on the nitration of tyrosine residues in mitochondrial complexes I, III, and V proteins in WT and MnSOD^{+++} mice. Mice killed 6 or 24 h after the administration of water served as pooled zero-time controls (0 h) for the LPS treatment. Other mice were killed 6 or 24 h after the LPS administration. Some WT mice were treated with Mito-TEMPO (50 mg/kg), UA (500 mg/kg), or 1400W (10 mg/kg) 30 min before and 8 h after LPS administration. **(A)** Equal amounts of liver mitochondrial proteins (35 μg) underwent blue native-gel electrophoresis (19) to separate intact oxidative phosphorylation complexes. **(B)** Separated complexes were transferred to nitrocellulose membranes for Western blot detection of 3-nitrotyrosine residues in the proteins of complex I, III, and V with an anti-3-nitrotyrosine antibody. Shown are representative gels of three independent experiments (19). (To see this illustration in color the reader is referred to the web version of this article at www.liebertonline.com/ars).

Peroxynitrite also damages lipids and proteins, causing nitrotyrosine formation, tyrosine oxidation, and loss of function (18). In the present study, LPS increased 3-nitrotyrosine residues in the proteins of mitochondrial complexes (Fig. 5B) and decreased respiratory complex I activity by 43% at 6 h (Fig. 2). This early dysfunction is unlikely to be due to decreased protein synthesis, as the expression of respiratory complex proteins (Fig. 5A) and that of the mtDNA-encoded COX2 protein (data not shown) were not modified 6 or 24 h after LPS administration. The rapid impairment of complex I activity is likely due to the oxidative damage inflicted to proteins and possibly unsaturated lipids by ROS, particularly peroxynitrite, as suggested by the protective effects of NOS inhibitors, a superoxide scavenger, and a peroxynitrite scavenger (Table 2). Impaired electron flow along the respiratory chain causes electrons to accumulate within chain components, and some of the accumulated electrons to react with oxygen to form superoxide, thus increasing mitochondrial superoxide formation (Fig. 13) (10). Therefore, the decreased respiratory complex I activity is likely to further enhance and sustain mitochondrial ROS formation (Fig. 13).

Another target for ROS- and peroxynitrite-mediated inactivation is MnSOD (2, 8, 27). Despite induction of the MnSOD mRNA (Fig. 3C), the protein level and activity of MnSOD decreased after LPS administration (Fig. 4), whereas Cu,Zn-SOD activity remained unchanged (Supplementary Fig. S3). Although Mito-TEMPO or uric acid prevented the LPS-mediated MnSOD decrease in WT mice (Fig. 4), MnSOD overexpression, albeit preventing many other effects of LPS (Figs. 5–7, 10, and 11), did not prevent the decrease in MnSOD protein after LPS administration (Fig. 4). Although further studies are required, these discrepancies could be consistent with mechanism-based enzyme destruction. The reduced MnSOD activity after LPS administration may further increase the intramitochondrial concentration of superoxide and its reaction with NO to form peroxynitrite (Fig. 13). Thus, several mechanisms may be involved in oxidative stress after LPS administration, including TNF-α, IFN-γ, and iNOS induction; respiratory chain impairment; and decreased MnSOD activity (Fig. 13). These redundant mechanisms could explain why preventing TNF-α secretion with pentoxifylline did not suffice to protect against LPS-induced mtDNA damage (Fig. 7).

In addition to TNF-α and IFN-γ, type I IFNs also increase after LPS administration (Fig. 9). *In vitro*, exposure of HUH7 cells to IFN-β for 2 h depleted COX2 mRNA (a mitochondrial transcript) without increasing ROS formation and without depleting mtDNA at this early time (Supplementary Fig. S6). The IFNs have been shown to suppress mtDNA gene transcription by activating RNase L, which may degrade the nDNA-encoded Tfam mRNA in the cytosol (Fig. 13) (23). In the present study, LPS decreased both Tfam mRNA and Tfam protein (Fig. 8), which could contribute, together with the mtDNA damage and mtDNA depletion caused by ROS/RNS, to a decreased synthesis rate of mitochondrial transcripts (Fig. 13). The RNase L is also expressed in mitochondria, where it degrades mtDNA-encoded mRNAs in a translation-dependent process, which is blocked by chloramphenicol, a

mitochondrial translation inhibitor (23). In the present study, chloramphenicol attenuated the LPS-induced decrease in ND1 and COX2 mRNAs 24 h after LPS administration, at a time when IFN-β was markedly induced (Fig. 9). These observations suggest that the translation-dependent degradation of mitochondrial transcripts by type I IFN-activated RNase L may contribute, at least in part, to the decrease in mitochondrial transcripts 24 h after LPS administration (Fig. 13).

Although the decrease in mitochondrial transcripts is unlikely to significantly contribute to early mitochondrial dysfunction as previously discussed, it could have a role in sustaining prolonged mitochondrial dysfunction as long as 48 h after LPS administration (Fig. 2). Although longer time periods were not investigated in the present study, previous studies have shown that increased PGC-1, NRF-1 and Tfam expression then drive increased mitochondrial biogenesis and mitochondrial function recovery 2–4 days after LPS administration (40–42).

Although only the liver was investigated in the present study, mitochondria in other organs could be affected as well. Indeed, mtDNA was depleted in the heart of LPS-treated animals (40), and in the liver, heart, skeletal muscle, and brain of ethanol-treated mice (30).

The present study mostly employed a dose of LPS (5 mg/kg) that was high enough to cause severe mitochondrial dysfunction but low enough not to kill the animals or cause severe liver lesions. A similar dissociation between severe dysfunction and relatively preserved histology can occur in septic patients. Severe multiorgan failure often contrasts with mild tissue lesions. Presumably, low ATP levels in high energy-consuming organs remain sufficient to perform housekeeping tasks and save the cells, although they are insufficient to ensure extraneous tasks such as maintaining efficient heart contractions, hepatic bile excretion, renal fluid secretion, or a normal level of consciousness. Our finding that severe LPS-induced mtDNA depletion, ATP depletion, protein nitrotyrosine formation, and ALT elevation is preventable in mice (Table 2 and Figs. 5, 6, and 10) and that LPS-induced mortality after a higher dose (25 mg/kg) can be delayed (Fig. 11) could raise hope that the dire prognosis of severe sepsis could perhaps be therapeutically improved in humans. However, further experimental studies are needed, both in the aseptic model used in the present study and in models based on living germs, such as the cecal ligation and puncture model, which also causes mitochondrial dysfunction (49).

Materials and Methods

Materials and chemicals

The MitoSOX Red reagent was from Invitrogen (Cergy Pontoise, France). The DHR123 and H_2DCF-DA were from Molecular Probes (Eugene, OR). The Mito-TEMPO was from Enzo Life Sciences (Villeurbanne, France). The mouse

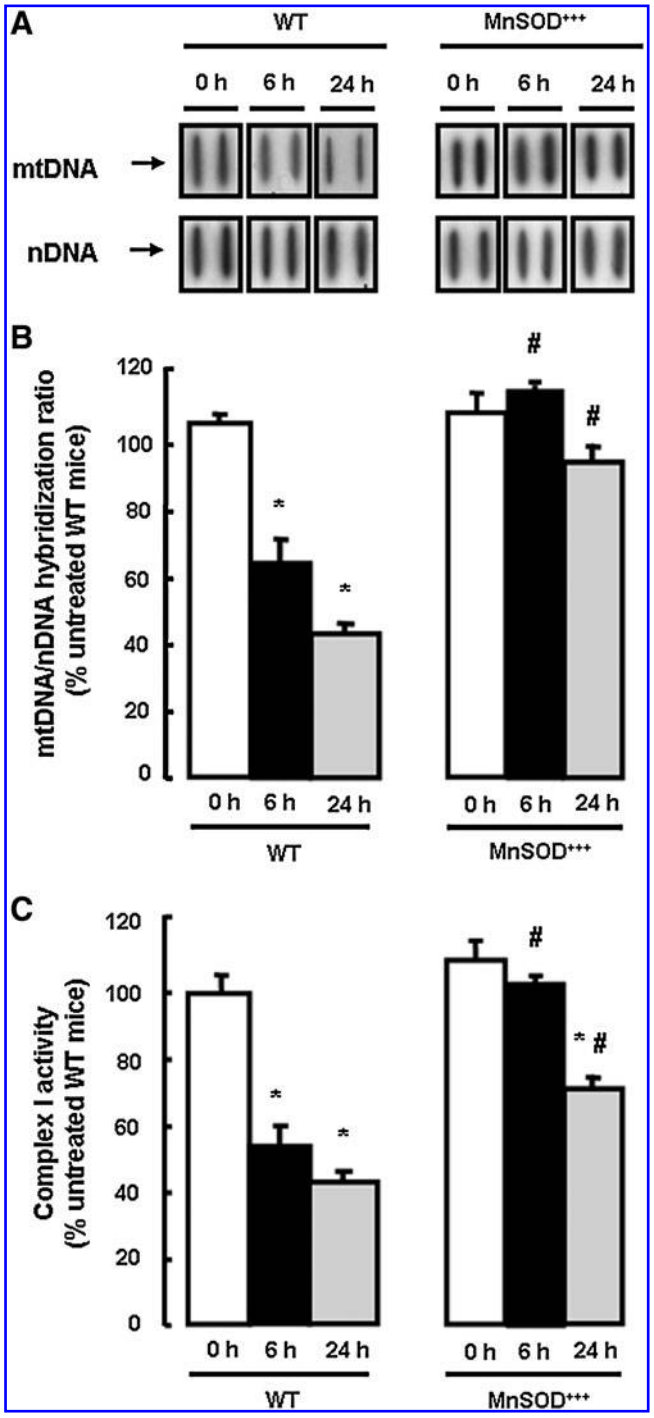

FIG. 6. MnSOD overexpression protected against LPS-induced mtDNA depletion and complex I impairment. The WT or MnSOD^{+++} mice killed 6 or 24 h after the administration of water served as pooled zero-time controls (0 h) for WT or MnSOD^{+++} mice sacrificed 6 or 24 h after LPS (5 mg/kg) administration. **(A)** Total hepatic DNA (300 ng) was blotted onto a nylon membrane, hybridized with a 10.9-kb mtDNA probe, stripped, and rehybridized with a mouse C_ot-1 nDNA probe. **(B)** For each mouse, blot intensities were determined by densitometry analysis, and the mtDNA/nDNA hybridization ratio was calculated and expressed as the percentage of the mean value for untreated mice. Data are expressed as mean ± SEM for 8–10 mice. **(C)** Complex I activity was assayed by following the oxidation of NADH in the presence of decylubiquinone and antimycin A. Results are expressed as mean ± SEM in six mice. *Different from untreated WT mice (0 h), $p < 0.05$. #Different from WT mice studied at the same treatment time (6 or 24 h) ($p < 0.05$, two-way ANOVA).

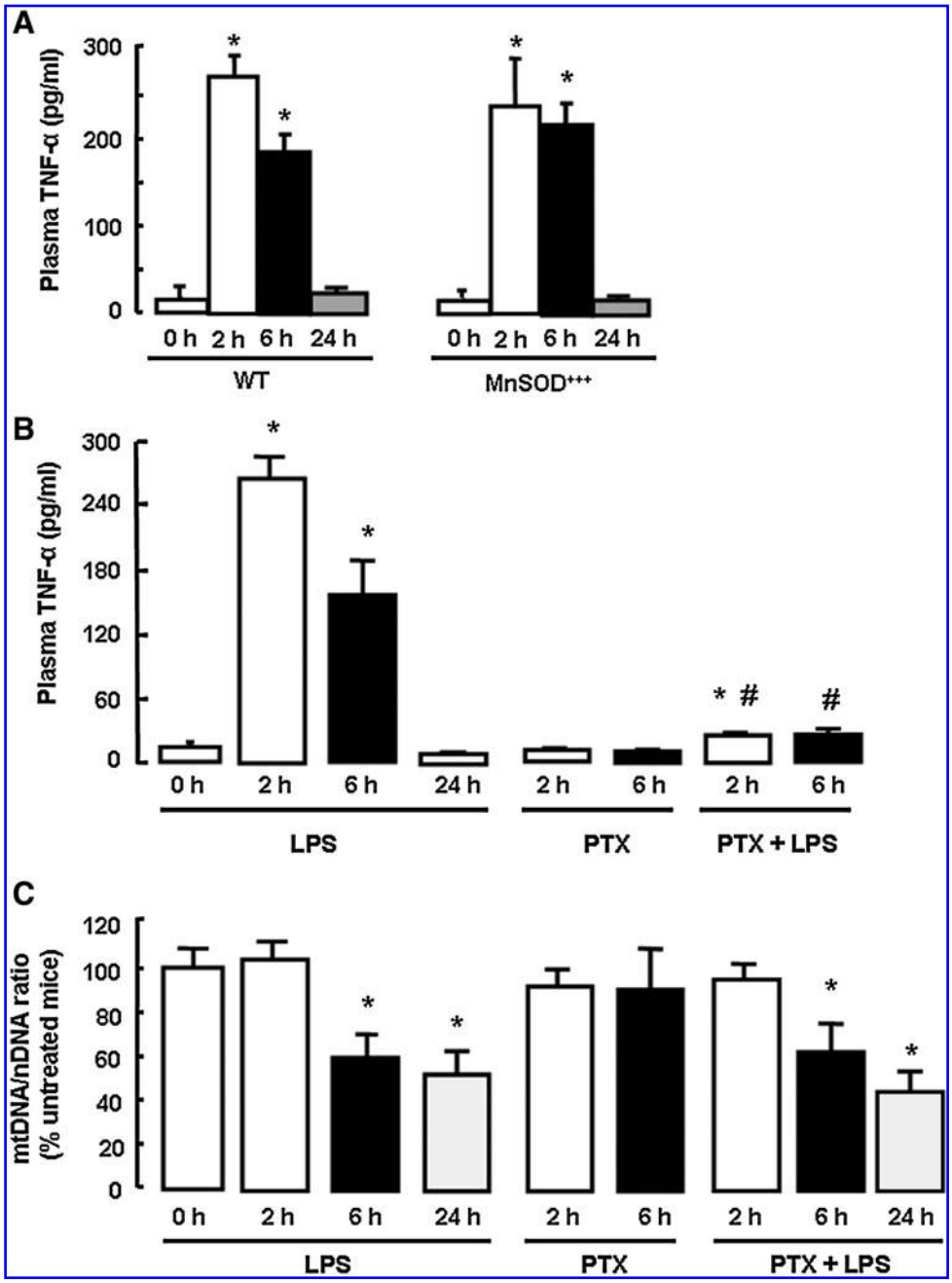

FIG. 7. Effects of LPS and/or pentoxifylline (PTX) on plasma tumor necrosis factor-alpha (TNF-α) and hepatic mtDNA levels. Mice killed 2, 6, or 24 h after the administration of water served as pooled zero-time controls (0 h) for mice sacrificed 6, 24 or 48 h after LPS (5 mg/kg) administration. The PTX (100 mg/kg body weight) was administered intraperitoneally (i.p.) first 30 min before and then 8 h after LPS administration. **(A)** Comparative plasma TNF-α levels in WT and MnSOD^{+++} mice. **(B)** Plasma TNF-α levels after LPS and or PTX administration in WT mice. **(C)** Hepatic mtDNA/nDNA hybridization ratios after LPS and/or PTX administration in WT mice. Results are expressed as mean ± SEM for 12 mice. *Different from untreated mice (0 h) ($p < 0.05$, one-way ANOVA). #Different from mice treated with LPS alone and studied at the same treatment time ($p < 0.05$, one-way ANOVA).

monoclonal antibody against iNOS was obtained from BD Transduction Laboratories (Le Pont de Claix, France). The mouse monoclonal antibody against COX2, the goat polyclonal antibody against Tfam, and the rabbit polyclonal antibodies against MnSOD and PGC-1 were all purchased from Tebu-Bio (Le Perray en Yvelines, France). The goat polyclonal antibody against C-terminal domains of TLR4 was from Santa Cruz Biotechnology Inc. (Santa Cruz, CA). The IFN-β was from PBL InterferonSource (Piscataway, NJ). The caspase-3 activity kit was purchased from Biomol (Plymouth Meeting, PA). Hybond-N$^+$ membranes, Hybond-C-extra membranes, and α-dCTP P^{32} were purchased from GE Healthcare (Orsay, France). The Expand Long Template PCR System was from Roche Applied Science (Mannheim, Germany). The LPS serotype 011:B4 and all other products were purchased from Sigma (St. Louis, MO).

Animals and treatments

The WT C57BL/6J mice from Janvier (Le Genest Saint Isle, France) were bred with transgenic mice overexpressing MnSOD (MnSOD^{+++}) as previously described (19). WT and MnSOD^{+++} mice were backcrossed into an inbred strain for at least 13 generations. Animals were fed a standard diet *ad libitum* (A04-10 biscuits; UAR, Villemoisson-sur-Orge, France). Animals received humane care, and all experiments were performed according to national guidelines for the use of animals in biomedical research. At 2 months of age (weight 28–32 g),

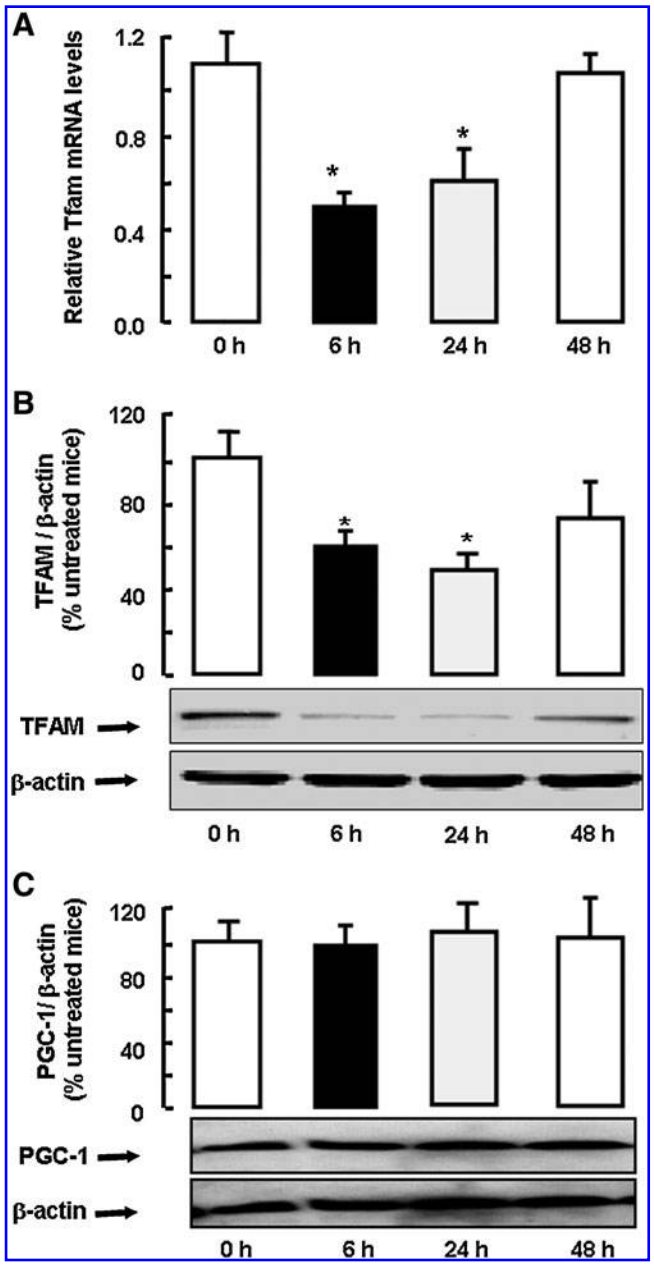

FIG. 8. Effects of LPS administration on mitochondrial transcription factor A (Tfam) and peroxisome proliferator-activated receptor gamma coactivator 1 (PGC-1) expression. The WT mice killed 6, 24, or 48 h after the administration of water served as pooled zero-time controls (0 h) for mice sacrificed 6, 24, or 48 h after LPS administration (5 mg/kg). **(A)** Hepatic RNA was reverse-transcribed, and cDNA underwent qRT-PCR with primers for Tfam and ribosomal protein S6 (S6). The relative to control Tfam mRNA expression was normalized to S6 mRNA. Results are expressed as mean ± SEM in 10 mice. **(B)** Hepatic proteins underwent SDS-PAGE and transfer to nitrocellulose membranes that were revealed with anti-Tfam or anti-β-actin antibodies. The Tfam protein/β-actin protein intensity ratio (mean ± SEM) was quantified in 10 mice. **(C)** Hepatic proteins underwent SDS-PAGE and transfer to nitrocellulose membranes that were revealed with anti-PGC-1 or anti-β-actin antibodies. The PGC-1 protein/β-actin protein intensity ratio (mean ± SEM) was quantified in 10 mice. *Different from untreated mice (0 h) ($p < 0.05$, one-way ANOVA).

$MnSOD^{+++}$ mice and/or their WT littermates were intraperitoneally (i.p.) injected either with water alone or with a homogeneously hazy solution of LPS (5 mg/kg body weight) dissolved in water. Animals were killed by cervical dislocation at 2, 6, 24, or 48 h after LPS or water administration. Some WT mice received a single dose of chloramphenicol (1 g/kg body weight, i.p.), a mitochondrial translation specific inhibitor (23), 30 min before LPS administration and were killed at 6 or 24 h after LPS injection. Other WT mice were treated i.p. with Mito-TEMPO (50 mg/kg body weight), a mitochondrial targeted superoxide scavenger (15), or with L-NAME (80 mg/kg body weight), a broad spectrum NOS inhibitor (34), N-[3-(aminomethyl)benzyl]acetamidine (1400W) (10 mg/kg body weight), a selective iNOS inhibitor (34), pentoxifylline (100 mg/kg body weight), which prevents TNF-α secretion (21), apocynin (20 mg/kg body weight), a NOX inhibitor (28), or the peroxynitrite scavenger (12), uric acid (500 mg/kg body weight; administered as a suspension in 0.8% saline). These ROS scavengers and enzyme inhibitors were administered 30 min before LPS administration in mice killed at 2 or 6 h after LPS, and both 30 min before and 8 h after LPS administration, in mice killed at 24 h, to prolong their biological effects.

mtDNA levels and mtDNA integrity

Slot-blot hybridization was used to look for mtDNA depletion (32). Hepatic DNA was isolated by the phenol/chloroform method, and 300 ng were blotted onto Hybond-N^+ nylon membranes. Membranes were hybridized with a 10.9-kb mtDNA probe (nucleotides 4964–15,896) generated by long PCR and labeled by random priming. Membranes were then stripped and hybridized with a mouse C_ot-1 nDNA probe (Invitrogen). The mtDNA and nDNA were assessed by densitometry analysis of autoradiographs. We also used qRT-PCR with primers specific for the COX2 gene to assess mtDNA levels with a second and independent method. Long PCR experiments were performed to detect mtDNA lesions hampering polymerase progress and altering replication (32). This long PCR technique is based on the amplification of a long (8636-bp) and a short (316-bp) mtDNA fragment. Forward primer A (5′-CGACAGCTAAGACCCAAACTGGG-3′; nucleotides 470–492) and backward primer B (5′-CCCATTT CTTCCCATTTCATTGGC-3′; nucleotides 785–762) amplified a 316-bp mtDNA fragment, whereas forward primer C (5′-TACTAGTCCGCGAGCCTTCAAAGC-3′; nucleotides 4964–4987) and backward primer D (5′-GGGTGATCTTTGTTTGC GGGT-3′; nucleotides 13,599–13,579) amplified an 8636-bp mtDNA fragment. The PCRs were performed with the Expand Long PCR system according to the manufacturer's instructions using 40 pmol of primers. The thermocycler profile included initial denaturation at 94°C for 2 min, 26 cycles of 95°C for 45 s, 61°C for 10 s and 68°C for 8 min, and final extension at 68°C for 7 min. The PCR products (20 μl) were separated on 1.6% agarose gels stained with ethidium bromide. Photographs were taken under ultraviolet transillumination, and scanned to determine the respective intensities of the 316- and 8636-bp PCR products.

Mitochondrial complex I activity and liver ATP contents

Hepatic mitochondria were isolated as previously described (11), and submitochondrial particles were prepared by two cycles of freezing/thawing. Complex I was assayed by following

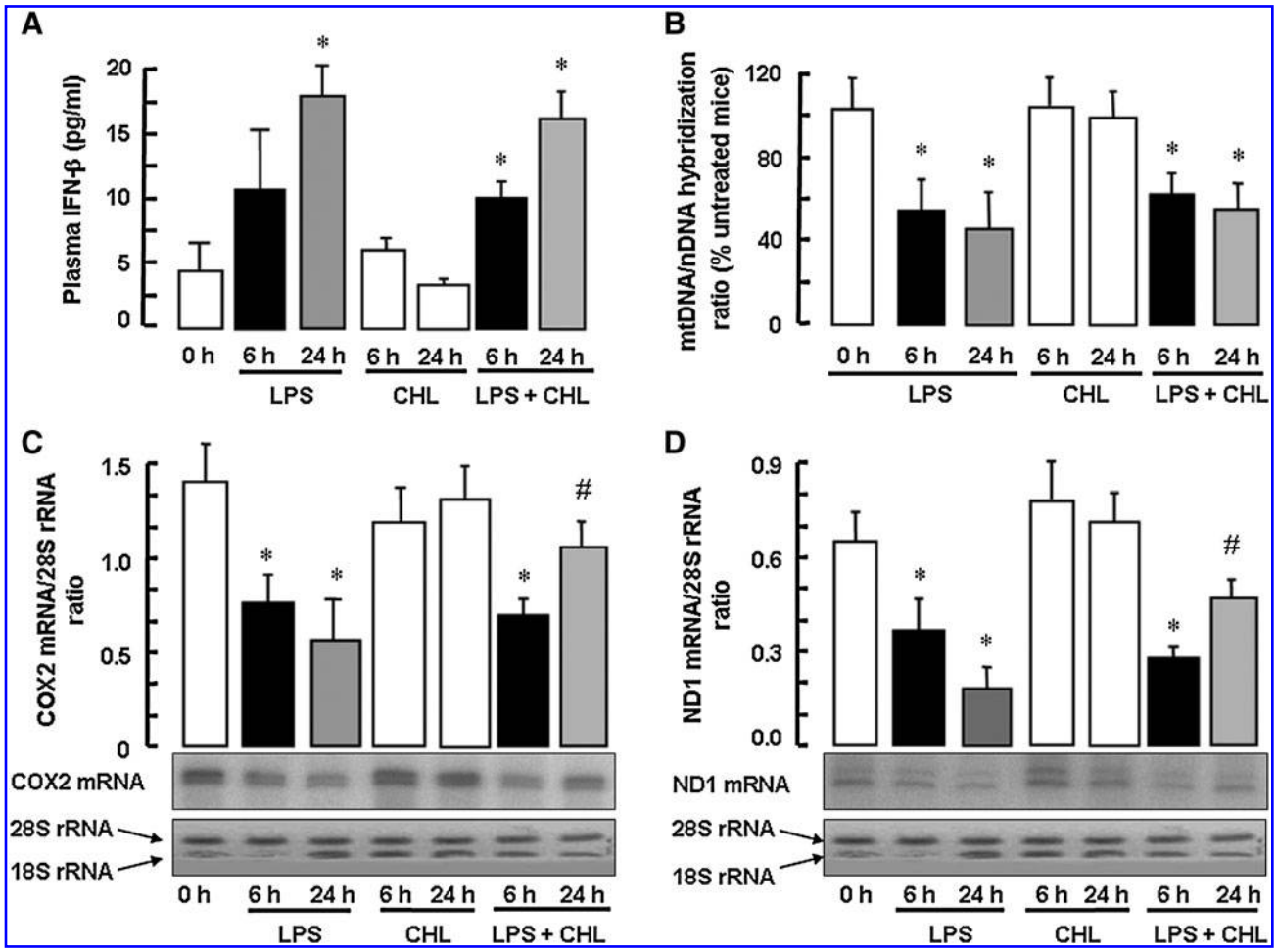

FIG. 9. Effects of LPS and/or chloramphenicol (CHL) on plasma interferon-β (IFN-β), mtDNA levels, and the mitochondrial mRNAs of subunit 2 of cytochrome *c* oxidase (COX2) and subunit 1 of NADH dehydrogenase (ND1). The WT mice killed 6 and 24 h after the administration of water served as pooled zero-time controls (0 h) for mice sacrificed 6 or 24 after LPS (5 mg/kg) administration. Some mice received an injection of CHL (1 g/kg body weight, i.p.) 30 min before LPS. Plasma IFN-β concentration **(A)** was determined by enzyme-linked immunosorbent assay. The mtDNA/nDNA hybridization ratio **(B)** was assessed by slot-blot hybridization. The mtDNA-encoded COX2 mRNA **(C)**, the mtDNA-encoded ND1 mRNA **(D)**, and the nDNA-encoded 28S rRNA **(C, D)** were assessed by Northern blot, and their mean intensity ratio was determined. Values are expressed as mean ± SEM for 5–12 mice. *Different from untreated mice (0 h) ($p < 0.05$, one-way ANOVA). #Different from mice treated with LPS alone and studied at the same treatment time ($p < 0.05$, one-way ANOVA).

the oxidation of NADH in the presence of decylubiquinone and antimycin A (36). To measure hepatic ATP, the liver was quickly excised and immediately ground in liquid nitrogen. The liver powder was transferred into 500 μl of ice-cold 1 *M* perchloric acid. After centrifugation at 4°C, 400-μl aliquots were neutralized with 5 *M* K_2CO_3 and centrifuged again at 4°C. The pellet was resuspended in phosphate-buffered saline (PBS) containing 0.2 N NaOH and used to determine protein content; the supernatant was used to measure ATP with a luciferine-luciferase assay kit following the manufacturer's recommendations (Roche Diagnostics, Mannheim, Germany).

Hepatic aconitase activity, mitochondrial ROS formation, and NOX activity

To assess hepatic aconitase activity, frozen liver fragments (20 mg) were homogenized in 500 μl of buffer containing 50 m*M* Tris HCl, pH 7.4, 0.2 m*M* sodium citrate, and 0.05 m*M* $MgCl_2$. Homogenates were centrifuged at 800 *g* at 4°C for 10 min, and supernatants were sonicated for 20 s. Proteins (200 μg) were incubated at 37°C for 5 min with 1 m*M* sodium citrate, 1 m*M* $NADP^+$, and 2 U isocitrate dehydrogenase. The formation of NADPH was measured from its absorption at 340 nm (36). To assess ROS formation, a liver homogenate and liver mitochondria were prepared after water or LPS administration, and incubated with 10 m*M* succinate or 5 m*M* each of malate and glutamate in the presence of either the MitoSOX Red reagent (Invitrogen), a mitochondria-targeted superoxide indicator, or H_2DCF-DA, which forms the green fluorescent 2′,7′-dichlorofluorescein (DCF) in the presence of hydrogen peroxide and other peroxides (19), or DHR123, a mitochondrial avid cationic dye oxidized by peroxynitrite and other ROS to rhodamine 123. Mitochondrial TBARs were measured as described (32). The NOX activity was evaluated by measuring the superoxide dismutase-inhibitable reduction of cytochrome *c* (0.5 m*M*) by a hepatic homogenate (1 mg protein/ml) incubated at room temperature for 30 min with NADPH (0.1 m*M*), with or without superoxide dismutase (200 U/ml).

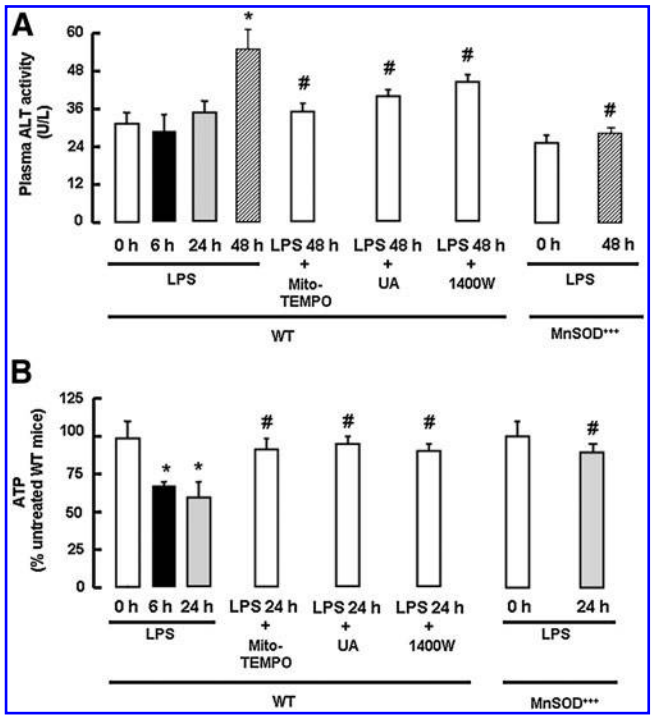

FIG. 10. Protective effects of MnSOD overexpression, Mito-TEMPO, UA, and 1400W against LPS-mediated changes in liver ATP at 24 h (B) and plasma alanine aminotransferase (ALT) at 48 h (A). The LPS (5 mg/kg) was administered to WT or MnSOD^{+++} mice. Some WT mice were treated with Mito-TEMPO (50 mg/kg), UA (500 mg/kg) or 1400W (10 mg/kg) 30 min before and 8 h after LPS administration. *Different from untreated mice (0 h), $p < 0.05$. #Different from WT mice treated with LPS alone and studied at the same treatment time (6, 24, or 48 h) ($p < 0.05$, two-way ANOVA).

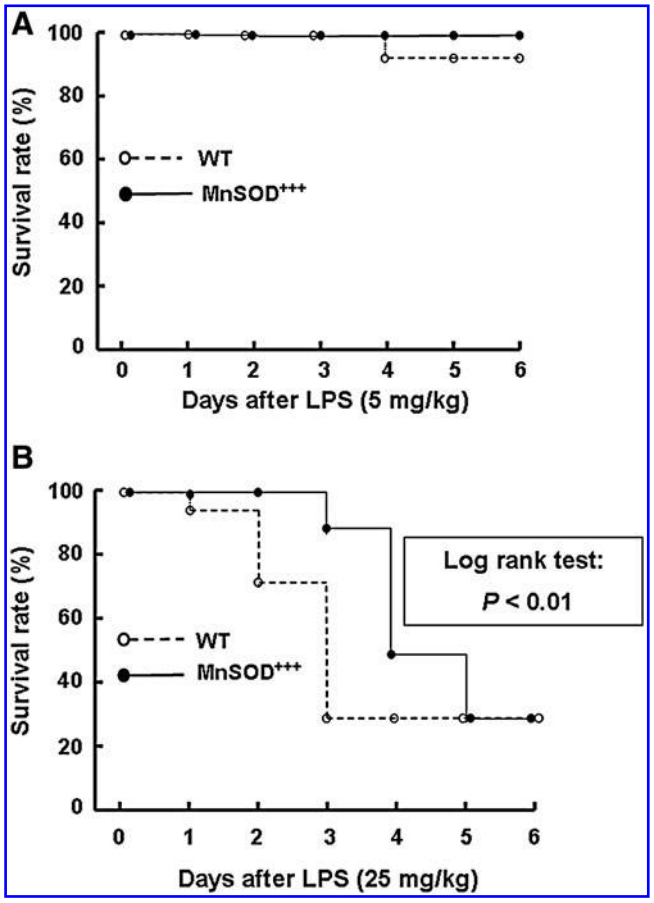

FIG. 11. MnSOD overexpression delayed death after administration of a high dose of LPS in mice. The WT mice and MnSOD^{+++} mice received LPS (5 or 25 mg/kg), and the survival rate of 25 mice per group was monitored daily for 6 days. The Kaplan-Meyer method was used to compare differences in mortality rates between groups. **(A)** LPS (5 mg/kg) and **(B)** LPS (25 mg/kg).

Plasma concentrations of nitrite/nitrate, TNF-α, IFN-β, IL-1β, HMGB1 and iron, and liver iron content

Blood was collected from the retro-orbitary sinus. Plasma nitrite/nitrate concentrations were determined with the Griess reaction (18). Plasma TNF-α and IL-1β were measured according to the manufacturer's instructions using a mouse TNF-α and IL-1β enzyme-linked immunosorbent assay (ELISA) kits from Invitrogen. The IFN-β was measured with a mouse IFN-β ELISA Kit from Santa Cruz Biotechnology. The HMGB1 was determined by ELISA using an HMGB1 antibody (ab 18256) from Abcam (San Francisco, CA). To measure liver iron, tissue underwent acid digestion as described (43), and iron content was measured on an Olympus AU400 automat using the OSR6186 kit (Olympus Diagnostic, Rungis, France). Plasma iron was assessed with the same method.

RNA isolation and qRT-PCR analysis of iNOS, MnSOD, Tfam, and COX2 mRNA expression

The RNA was purified from livers using the TRIzol® reagent (Invitrogen). Reverse transcription was performed with 2 μg of total RNA in a reaction buffer containing 20 m*M* Tris-HCl (pH 8.3), 375 m*M* KCl, 15 m*M* MgCl2, 10 m*M* dithiothreitol, 0.5 m*M* of each deoxynucleoside triphosphate, 250 ng of random primers, 2 U RNase inhibitor, and 10 U Moloney murine leukemia virus reverse transcriptase. The reaction was carried out at 37°C for 50 min, and the mixture was heated at 70°C for 15 min. The qRT-PCR was performed on an 5-μl aliquot of the reverse transcription reaction with 0.25 μM of each primer (Table 3) and 10 μl of Master SYBR Green Mix (Sigma) on a Chromo IV light cycler apparatus (Bio-Rad, Marne-La-Coquette, France). The PCR conditions were one cycle at 94°C for 3 min followed by 40 cycles at 94°C for 30 s and 60°C for 1 min. Amplification of transcripts was confirmed by a melting curve generated at the end of each run. The PCR specificity was further ascertained by checking the size of the PCR products on agarose gels. Controls (no DNA template) were run to ensure that there was no amplification of contaminating DNA. Expression of the mouse ribosomal protein S6 (S6) was used as the reference gene. The $2^{-\Delta\Delta Ct}$ method was used to express relative Tfam, iNOS, MnSOD, and COX2 expression normalized to S6.

Hepatic MnSOD and Cu,ZnSOD activities

Native gel assays were used to assess MnSOD and Cu,ZnSOD activities (19). Total hepatic proteins (100 μg) were

resuspended in 40% glycerol and 0.025% bromophenol blue, and loaded on a nondenaturing 15% polyacrylamide gel. Migration was performed at 4°C for 12 h at 120 V, and superoxide dismutase activity was assessed within the gel, as described (19).

Northern blot hybridization assay for COX2 and ND1 mRNAs

Ten-microgram aliquots of RNA were denatured for 10 min at 65°C in 61.5% deionized formamide, 19.6% formaldehyde, and 5% glycerol "Northern buffer" (10 × stock: 0.5 *M* boric acid, 50 m*M* sodium borate, 100 m*M* sodium sulfate, and 10 m*M* EDTA, pH 8.0). Samples were rapidly cooled and subjected to electrophoresis in 1% agarose-formaldehyde. The RNA was blotted onto Hybond-N^+ nylon filters. Filters were hybridized overnight at 65°C in a solution containing the radiolabeled probe and single-stranded salmon sperm DNA. The probe for mitochondrial COX2 mRNA extended from nucleotide 5454 to nucleotide 7720 of the mouse mtDNA; that for NDl, ranged from nucleotide 3102 to nucleotide 3803. After hybridization, filters were first washed twice for 30 min at room temperature in 1% sodium dodecyl sulfate (SDS), 0.25 *M* phosphate buffer, and then thrice for 30 min at 65°C in 0.1% SDS, 0.40 *M* phosphate buffer. Signals were detected with an Instant Imager.

Western blot analysis of Tfam, PGC-1, iNOS, MnSOD, and COX2

To assess protein expression, equal amounts of total liver proteins (50 μg) were separated by SDS-polyacrylamide gel electrophoresis, and transferred onto nitrocellulose membranes. Membranes were blocked and incubated overnight at 4°C with an antibody against MnSOD, iNOS, Tfam, PGC-1, or COX2. After three washings with PBS, membranes were incubated for 1 h at room temperature with an appropriate horseradish peroxidase-conjugated secondary antibody (1:10,000 dilution) in PBS containing 0.05% Tween 20. Blots were stained with the enhanced chemiluminescence method, and exposed to an X-ray film. Blots were stripped and exposed to an anti-β-actin antibody. Protein bands were quantified by densitometry.

Liver morphology, ALT activity, caspase-3 activity, and assay for nDNA fragmentation

A liver fragment for light microscopy was fixed with 10% formalin in PBS, dehydrated in an alcoholic series, placed in

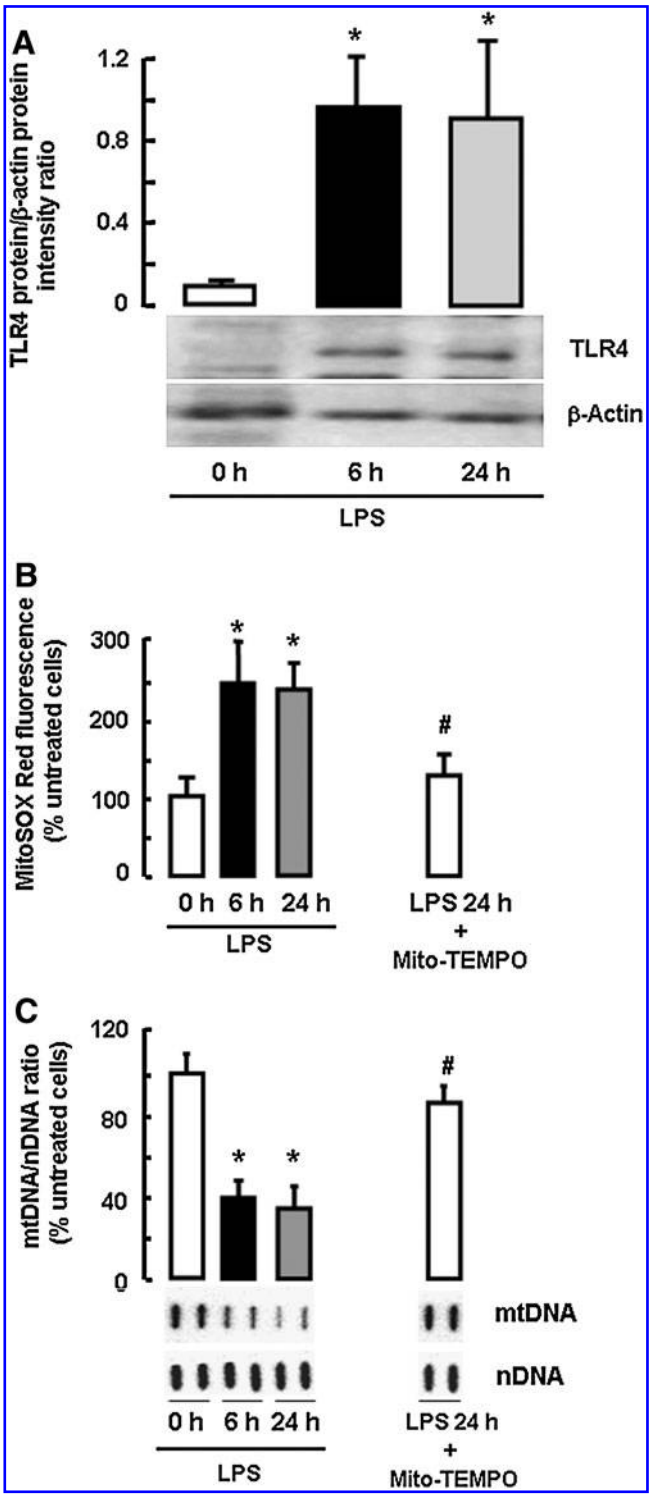

FIG. 12. Effect of LPS on Toll-like receptor 4 (TLR4) protein expression, mitochondrial superoxide production, and mtDNA content in HepG2 cells. The HepG2 cells (4×10^5 cells/ml) were incubated for 6 or 24 h with or without LPS (5 μM) in Dulbecco's modified Eagle's medium. **(A)** Total proteins underwent SDS-PAGE and transfer to nitrocellulose membranes that were revealed with anti-TLR4 or anti-β-actin antibodies. The TLR4 protein/β-actin protein intensity ratio (mean ± SEM) was quantified ($n = 3$ determinations). **(B)** The HepG2 cells were plated in 96-well plates and incubated with or without LPS (5 μM) and Mito-TEMPO (10 μg/ml). Six or 24 h later, MitoSOX Red (5 μM) was added to the cells and incubated for an additional 10 min at 37°C. The MitSOX Red fluorescence was then recorded at Extinction/Emission 510/520 nm. **(C)** Total DNA (300 ng) was extracted and blotted onto a nylon membrane. The DNA was hybridized with a human mtDNA probe, stripped, and rehybridized with a human C_ot-1 nDNA probe. For each cell culture dish, blot intensities were determined by densitometry analysis, and the mtDNA/nDNA hybridization ratio was calculated and expressed as the percentage of the mean value for untreated cells (0 h). Values represent means ± SEM for six determinations. *Different from untreated cells (0 h), $p < 0.05$. #Different from cells treated with LPS alone and studied at 24 h, $p < 0.05$.

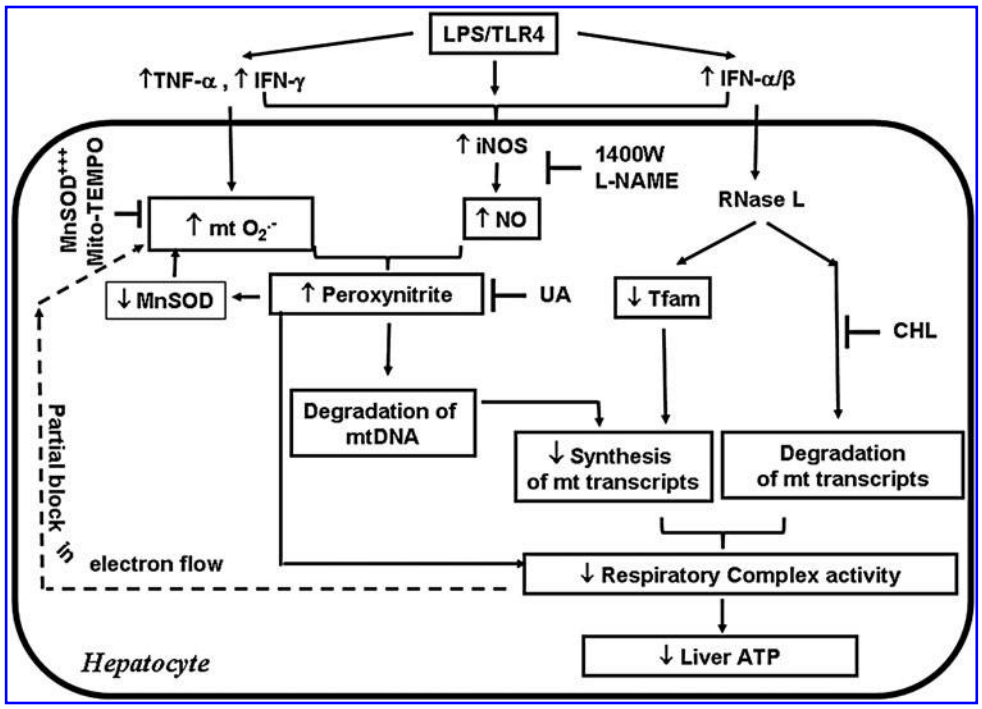

FIG. 13. Suggested mechanisms for LPS-induced mitochondrial dysfunction. The LPS/TLR4 interaction on the surface of Kupffer cells increases the secretion of TNF-α and IFNs, and triggers an increased iNOS expression in hepatocytes. The TNF-α, IFN-γ, and possibly other mechanisms increase mitochondrial (mt) superoxide ($O_2^{\cdot -}$) formation, whereas the induced iNOS synthesizes increased amounts of NO. The conjunction of an increased mitochondrial superoxide production with an increased NO formation should increase the formation of peroxynitrite that damages mtDNA (thus leading to mtDNA degradation by mitochondrial endonucleases), MnSOD (thus further increasing superoxide concentration and peroxynitrite formation), and complex I proteins (thus decreasing complex I activity, which should partially block the flow of electrons, and increase their reaction with oxygen to form superoxide). Concomitantly, IFN-α/β activates RNase L, which degrades both Tfam mRNA and mitochondrial transcripts. Albeit not responsible for early effects (6 h), the decreased transcripts could help sustain mitochondrial dysfunction 48 h after LPS administration. The suggested site of action of the protective compounds Mito-TEMPO, MnSOD, UA, 1400W, nitro-L-arginine methyl ester (L-NAME), and CHL are shown.

toluene baths, and embedded in paraffin. Sections (3-μm thick) were prepared for hematoxylin and eosin staining. The ALT activity was measured with the Enzyline ALAT/GPT kit (Biomérieux, Marcy l'Etoile, France). For the caspase-3 activity assay, livers were minced and homogenized in 1 m*M* EDTA, 50 m*M* Hepes, 0.1% 3-[(3-cholamidopropyl)dimethylammonio)-1-propane-sulfonate, 5 m*M* dithiothreitol, 4 mg/ml leupeptin, and 4 mg/ml pepstatin, pH 7.4. After centrifugation at 14,000 *g*, caspase-3 activity was measured in the supernatant with a fluorescent assay kit (Biomol) (19). We looked for nDNA fragmentation using the sensitive C_ot-1 hybridization technique (32). Briefly, hepatic DNA was separated on 2% agarose gels and transferred to a nylon membrane (Hybond-N^+). Membranes were hybridized with mouse C_ot-1 nDNA probe labeled by random priming (32).

Table 3. Mouse Gene-Specific Oligonucleotide Sequences Used in Quantitative Real-Time Polymerase Chain Reaction

Gene product	*Primer sequences*
Tfam	FW: 5′-GGCCAAGGGAGATGTTACAA-3′
	RV: 5′-GCTTGATAGCCTCCAGCAAC-3′
iNOS	FW: 5′-GGGCAAACATCACATTCAGATCCCG-3′
	RV: 5′-ATATTGCTGTGGCTCCCATGTT-3′
MnSOD	FW: 5′-TTAACGCGCAGATCATGCA-3′
	RV: 5′-GGTGGCGTTGAGATTGTTCA-3′
S6	FW: 5′-TGTCCGCCAGTATGTTGTCAGGAAG-3′
	RV: 5′-TGCTTTGGTCCTGGGCTTCTTACC-3′
COX2	FW: 5′-GATAACCGAGTCGTTCTGCCA-3′
	RV: 5′-CCCTGGTCGGTTTGATGTTAC-3′

Tfam, mitochondrial transcription factor A; iNOS, inducible nitric oxide synthase; MnSOD, manganese superoxide dismutase; S6, mouse ribosomal protein S6; COX2, subunit 2 of cytochrome *c* oxidase; FV, forward; RV, reverse.

Culture of human hepatic cell lines

The human hepatoma HepG2 and HuH7 cell lines were purchased from ATCC (Rockville, MD) and Japan Health Research Resources Bank (Osaka, Japan), respectively. Cells were cultured at 37°C in a 5% CO_2/95% air atmosphere in Dulbecco's modified Eagle's medium supplemented with 10% fetal calf serum, streptomycin (0.1 mg/ml) and penicillin (100 U/ml).

Statistical analysis

Since the different parameters investigated were similar in mice sacrificed either 2, 6, 24, or 48 h after water administration, these mice were pooled into a single group and served as zero-time controls (designed as "0 h") for mice sacrificed 2, 6, 24, or 48 h after LPS administration. We used one-way analysis of variance (ANOVA) tests followed by Fisher's protected least significant difference (PLSD) tests to assess the effects of the LPS treatment.

In some experiments, where we used both WT mice and $MnSOD^{+++}$ transgenic mice, we applied two-way ANOVA to assess the mitochondrial effects of the MnSOD genotype, the LPS treatment, and their interactions. The means of diverse groups were then compared with Fisher's PLSD *post hoc*

tests. Values were expressed as means ± standard error of the mean, and the significance level was set at $p < 0.05$. The Kaplan-Meyer log-rank method were used to compare the differences in survival rates between groups. The chi-square test (χ^2) or the chi-square test corrected for continuity (χ^{c2}) was used to assess differences between frequencies of LPS-induced liver histology lesions.

Acknowledgments

The authors thank Prof. D. Henin (Laboratoire d'Anatomo-Pathologie, Hôpital Bichat, France) for assessing liver lesions. Amal Choumar has been a recipient of fellowship from Fondation pour la Recherche Médicale.

Author Disclosure Statement

No competing financial interests exist.

References

1. Bailey SM, Mantena SK, Millender-Swain T, Cakir Y, Jhala NC, Chhieng D, Pinkerton KE, and Ballinger SW. Ethanol and tobacco smoke increase hepatic steatosis and hypoxia in the hypercholesterolemic apoE(-/-) mouse: implications for a "multihit" hypothesis of fatty liver disease. *Free Radic Biol Med* 46: 928–938, 2009.
2. Barreiro E, Sánchez D, Gáldiz JB, Hussain SN, and Gea J; ENIGMA in COPD project. N-acetylcysteine increases manganese superoxide dismutase activity in septic rat diaphragms. *Eur Respir J* 26: 1032–1039, 2005.
3. Chau CM, Evans MJ, and Scarpulla RC. Nuclear respiratory factor 1 activation sites in genes encoding the gamma-subunit of ATP synthase, eukaryotic initiation factor 2 alpha, and tyrosine aminotransferase. Specific interaction of purified NRF-1 with multiple target genes. *J Biol Chem* 267: 6999–7006, 1992.
4. Coleman WB and Cunningham CC. Effects of chronic ethanol consumption on the synthesis of polypeptides encoded by the hepatic mitochondrial genome. *Biochim Biophys Acta* 1019: 142–150, 1990.
5. Cover C, Mansouri A, Knight TR, Bajt ML, Lemasters JJ, Pessayre D, and Jaeschke H. Peroxynitrite-induced mitochondrial and endonuclease-mediated nuclear DNA damage in acetaminophen hepatotoxicity. *J Pharmacol Exp Ther* 315: 879–887, 2005.
6. Cuzzocrea S, Mazzon E, Di Paola R, Esposito E, Macarthur H, Matuschak GM, and Salvemini D. A role for nitric oxide-mediated peroxynitrite formation in a model of endotoxin-induced shock. *J Pharmacol Exp Ther* 319: 73–81, 2006.
7. De Leo ME, Landriscina M, Palazzotti B, Borrello S, and Galeotti T. Iron modulation of LPS-induced manganese superoxide dismutase gene expression in rat tissues. *FEBS Lett* 403: 131–135, 1997.
8. Demicheli V, Quijano C, Alvarez B, and Radi R. Inactivation and nitration of human superoxide dismutase (SOD) by fluxes of nitric oxide and superoxide. *Free Radic Biol Med* 42: 1359–1368, 2007.
9. Epe B, Ballmaier D, Roussyn I, Briviba K, and Sies H. DNA damage by peroxynitrite characterized with DNA repair enzymes. *Nucleic Acids Res* 24: 4105–4110, 1996.
10. Esposito LA, Melov S, Panov A, Cottrell BA, and Wallace DC. Mitochondrial disease in mouse results in increased oxidative stress. *Proc Natl Acad Sci U S A* 96: 4820–4825, 1999.
11. Fisch C, Robin MA, Lettéron P, Fromenty B, Berson A, Renault S, Chachaty C, and Pessayre D. Cell-generated nitric oxide inactivates rat hepatocyte mitochondria *in vitro* but reacts with hemoglobin *in vivo. Gastroenterology* 110: 210–220, 1996.
12. García-Ruiz I, Rodríguez-Juan C, Díaz-Sanjuan T, del Hoyo P, Colina F, Muñoz-Yagüe T, and Solís-Herruzo JA. Uric acid and anti-TNF antibody improve mitochondrial dysfunction in ob/ob mice. *Hepatology* 44: 581–591, 2006.
13. Goossens V, Grooten J, De Vos K, and Fiers W. Direct evidence for tumor necrosis factor-induced mitochondrial reactive oxygen intermediates and their involvement in cytotoxicity. *Proc Natl Acad Sci U S A* 92: 8115–8119, 1995.
14. Inagaki H, Matsushima Y, Ohshima M, and Kitagawa Y. Interferons suppress mitochondrial gene transcription by depleting mitochondrial transcription factor A (mtTFA). *J Interferon Cytokine Res* 17: 263–269, 1997.
15. Jiang A, Stoyanovsky DA, Belikova NA, Tyurina YY, Zhao Q, Tungekar MA, Kapralova V, Huang Z, Mintz AH, Greenberger JS, and Kagan VE. A mitochondria-targeted triphenylphosphonium-conjugated nitroxide functions as a radioprotector/metigator. *Radiat Res* 172: 706–717, 2009.
16. Kang D, Kim SH, and Hamasaki N. Mitochondrial transcription factor A (TFAM): roles in maintenance of mtDNA and cellular functions. *Mitochondrion* 7: 39–44, 2007.
17. Kang YH, Lee CH, Monroy RL, Dwivedi RS, Odeyale C, and Newball HH. Uptake, distribution and fate of bacterial lipopolysaccharides in monocytes and macrophages: an ultrastructural and functional correlation. *Electron Microsc Rev* 5: 381–419, 1992.
18. Koch OR, De Leo ME, Borrello S, Palombini G, and Galeotti T. Ethanol treatment up-regulates the expression of mitochondrial manganese superoxide dismutase in rat liver. *Biochem Biophys Res Commun* 201: 1356–1365, 1994.
19. Larosche I, Lettéron P, Berson A, Fromenty B, Huang TT, Moreau R, Pessayre D, and Mansouri A. Hepatic mitochondrial DNA depletion after an alcohol binge in mice: probable role of peroxynitrite and modulation by manganese superoxide dismutase. *J Pharmacol Exp Ther* 332: 886–897, 2010.
20. Larsson NG, Wang J, Wilhelmsson H, Oldfors A, Rustin P, Lewandoski M, Barsh GS, and Clayton DA. Mitochondrial transcription factor A is necessary for mtDNA maintenance and embryogenesis in mice. *Nat Genet* 18: 231–236, 1998.
21. Lebrec D, Thabut D, Oberti F, Perarnau JM, Condat B, Barraud H, Saliba F, Carbonell N, Renard P, Ramond MJ, Moreau R, and Poynard T; Pentocir Group. Pentoxifylline does not decrease short-term mortality but does reduce complications in patients with advanced cirrhosis. *Gastroenterology* 138: 1755–1762, 2010.
22. Leone TC, Lehman JJ, Finck BN, Schaeffer PJ, Wende AR, Boudina S, Courtois M, Wozniak DF, Sambandam N, Bernal-Mizrachi C, Chen Z, Holloszy JO, Medeiros DM, Schmidt RE, Saffitz JE, Abel ED, Semenkovich CF, and Kelly DP. PGC-1alpha deficiency causes multi-system energy metabolic derangements: muscle dysfunction, abnormal weight control and hepatic steatosis. *PLoS Biol* 3: e101, 2005.
23. Le Roy F, Silhol M, Salehzada T, and Bisbal C. Regulation of mitochondrial mRNA stability by RNase L is translation-dependent and controls IFNalpha-induced apoptosis. *Cell Death Differ* 14: 1406–1413, 2007.
24. Lin J, Tarr PT, Yang R, Rhee J, Puigserver P, Newgard CB, and Spiegelman BM. PGC-1beta in the regulation of hepatic glucose and energy metabolism. *J Biol Chem* 278: 30843–30848, 2003.

25. Liochev SI and Fridovich I. The effects of superoxide dismutase on H2O2 formation. *Free Radic Biol Med* 42: 1465–1469, 2007.
26. Liu P, McGuire GM, Fisher MA, Farhood A, Smith CW, and Jaeschke H. Activation of Kupffer cells and neutrophils for reactive oxygen formation is responsible for endotoxin-enhanced liver injury after hepatic ischemia. *Shock* 3: 56–62, 1995.
27. Macmillan-Crow LA and Cruthirds DL. Invited review: manganese superoxide dismutase in disease. *Free Radic Res* 34: 325–336, 2001.
28. Maldonado PD, Molina-Jijón E, Villeda-Hernández J, Galván-Arzate S, Santamaría A, and Pedraza-Chaverrí J. NAD(P)H oxidase contributes to neurotoxicity in an excitotoxic/prooxidant model of Huntington's disease in rats: protective role of apocynin. *J Neurosci Res* 88: 620–629, 2010.
29. Malyshev E, Tazi KA, Moreau R, and Lebrec D. Discrepant effects of inducible nitric oxide synthase modulation on systemic and splanchnic endothelial nitric oxide synthase activity and expression in cirrhotic rats. *J Gastroenterol Hepatol* 22: 2195–2201, 2007.
30. Mansouri A, Demeilliers C, Amsellem S, Pessayre D, and Fromenty B. Acute ethanol administration oxidatively damages and depletes mitochondrial DNA in mouse liver, brain, heart, and skeletal muscles: protective effects of antioxidants. *J Pharmacol Exp Ther* 298: 737–743, 2001.
31. Mansouri A, Fromenty B, Berson A, Robin MA, Grimbert S, Beaugrand M, Erlinger S, and Pessayre D. Multiple hepatic mitochondrial DNA deletions suggest premature oxidative aging in alcoholics. *J Hepatol* 27: 96–102, 1997.
32. Mansouri A, Gaou I, de Kerguenec C, Amsellem S, Haouzi D, Berson A, Moreau A, Feldmann G, Letteron P, Pessayre D, and Fromenty B. An alcoholic binge causes massive degradation of hepatic mitochondrial DNA in mice. *Gastroenterology* 117: 181–190, 1999.
33. McCulloch V, Seidel-Rogol BL, and Shadel GS. A human mitochondrial transcription factor is related to RNA adenine methyltransferases and binds S-adenosylmethionine. *Mol Cell Biol* 22: 1116–1125, 2002.
34. McKim SE, Gabele E, Isayama F, Lambert JC, Tucker LM, Wheeler MD, Connor HD, Mason RP, Doll MA, Hein DW, and Arteel GE. Inducible nitric oxide synthase is required in alcohol-induced liver injury: studies with knockout mice. *Gastroenterology* 125: 1834–1844, 2003.
35. Negishi M, Izumi Y, Aleemuzzaman S, Inaba N, and Hayakawa S. Lipopolysaccharide (LPS)-induced interferon (IFN)-gamma production by decidual mononuclear cells (DMNC) is interleukin (IL)-2 and IL-12 dependent. *Am J Reprod Immunol* 65: 20–27, 2011.
36. Puerta E, Hervias I, Goñi-Allo B, Zhang SF, Jordán J, Starkov AA, and Aguirre N. Methylenedioxymethamphetamine inhibits mitochondrial complex I activity in mice: a possible mechanism underlying neurotoxicity. *Br J Pharmacol* 160: 233–245, 2010.
37. Radi R, Cassina A, Hodara R, Quijano C, and Castro L. Peroxynitrite reactions and formation in mitochondria. *Free Radic Biol Med* 33: 1451–1464, 2002.
38. Scarpulla RC. Nuclear control of respiratory chain expression in mammalian cells. *J Bioenerg Biomembr* 29: 109–119, 1997.
39. Schoenberg MH, Weiss M, and Radermacher P. Outcome of patients with sepsis and septic shock after ICU treatment. *Langenbecks Arch Surg* 383: 44–48, 1998.
40. Suliman HB, Sweeney TE, Withers CM, and Piantadosi CA. Co-regulation of nuclear respiratory factor-1 by NF{kappa}B and CREB links LPS-induced inflammation to mitochondrial biogenesis. *J Cell Sci* 123(Pt 15): 2565–2575, 2010.
41. Suliman HB, Welty-Wolf KE, Carraway M, Tatro L, and Piantadosi CA. Lipopolysaccharide induces oxidative cardiac mitochondrial damage and biogenesis. *Cardiovasc Res* 64: 279–288, 2004.
42. Suliman HB, Welty-Wolf KE, Carraway MS, Schwartz DA, Hollingsworth JW, and Piantadosi CA. Toll-like receptor 4 mediates mitochondrial DNA damage and biogenic responses after heat-inactivated *E. coli*. *FASEB J* 19: 1531–1533, 2005.
43. Torrance JD and Bothwell TH. A simple technique for measuring storage iron concentrations in formalinised liver samples. *S Afr J Med Sci* 33: 9–11, 1968.
44. Víctor VM, Espulgues JV, Hernández-Mijares A, and Rocha M. Oxidative stress and mitochondrial dysfunction in sepsis: a potential therapy with mitochondria-targeted antioxidants. *Infect Disord Drug Targets* 9: 376–389, 2009.
45. Wallace DC. Mitochondrial diseases in man and mouse. *Science* 283: 1482–1488, 1999.
46. Watanabe Y, Suzuki O, Haruyama T, and Akaike T. Interferon-gamma induces reactive oxygen species and endoplasmic reticulum stress at the hepatic apoptosis. *J Cell Biochem* 89: 244–253, 2003.
47. Wieland P and Lauterburg BH. Oxidation of mitochondrial proteins and DNA following administration of ethanol. *Biochem Biophys Res Commun* 213: 815–819, 1995.
48. Yakes FM and Van Houten B. Mitochondrial DNA damage is more extensive and persists longer than nuclear DNA damage in human cells following oxidative stress. *Proc Natl Acad Sci U S A* 94: 514–519, 1997.
49. Zapelini PH, Rezin GT, Cardoso MR, Ritter C, Klamt F, Moreira JC, Streck EL, and Dal-Pizzol F. Antioxidant treatment reverses mitochondrial dysfunction in a sepsis animal model. *Mitochondrion* 8: 211–218, 2008.
50. Zhu H, Shan L, Schiller PW, Mai A, and Peng T. Histone deacetylase-3 activation promotes tumor necrosis factor-alpha (TNF-alpha) expression in cardiomyocytes during lipopolysaccharide stimulation. *J Biol Chem* 285: 9429–9436, 2010.

Address correspondence to:
Dr. Abdellah Mansouri
INSERM U773
Faculté de Médecine Xavier Bichat
16 rue Henri Huchard, BP 416
Paris 75018
France

E-mail: abdel.mansouri@inserm.fr

Date of first submission to ARS Central, November 3, 2010; date of final revised submission, June 1, 2011; date of acceptance, June 6, 2011.

Abbreviations Used

ALT = alanine amino transferase
ANOVA = analysis of variance
ATP = adenosine triphosphate
CHL = chloramphenicol
COX2 = subunit 2 of cytochrome *c* oxidase
Cu,ZnSOD = copper-zinc superoxide dismutase
DCF = 2′,7′-dichlorofluorescein

DHR123 = dihydrorhodamine 123
DMEM = Dulbecco's modified Eagle's medium
EDTA = ethylenediaminetetraacetic acid
ELISA = enzyme-linked immunosorbent assay
H_2DCF-DA = 2′,7′-dichlorodihydrofluorescein diacetate
HMGB1 = high-mobility group protein box-1
IFN-α, -β or -γ = interferon-α, -β, or -γ
IL-1β = interleukin-1β
iNOS = inducible nitric oxide synthase
i.p. = intraperitoneally
L-NAME = nitro-L-arginine methyl ester
LPS = lipopolysaccharide
Mito-TEMPO = (2-(2,2,6,6-tetramethylpiperidin-1-oxyl-4-ylamino)-2-oxoethyl)triphenylphosphonium chloride, monohydrate
MnSOD = manganese superoxide dismutase
$MnSOD^{+++}$ mice = MnSOD-overexpressing transgenic mice
mtDNA = mitochondrial DNA
NADH = reduced nicotinamide-adenine dinucleotide
$NADP^+$ = oxidized nicotinamide-adenine dinucleotide phosphate
NADPH = reduced nicotinamide-adenine dinucleotide phosphate
ND1 = subunit 1 of NADH dehydrogenase
nDNA = nuclear DNA
NOS = nitric oxide synthase
NOX = NADPH oxidase
NRF-1 or NFR-2 = nuclear respiratory factor-1 or -2
OXPHOS = oxidative phosphorylation system
PAGE = polyacrylamide gel electrophoresis
PBS = phosphate-buffered saline
PGC-1 = peroxisome proliferator-activated receptor gamma coactivator 1
PLSD = protected least significance difference
PTX = pentoxifylline
qRT-PCR = quantitative real-time polymerase chain reaction
RNS = reactive nitrogen species
ROS = reactive oxygen species
S6 = mouse ribosomal protein S6
SDS = sodium dodecyl sulfate
SEM = standard error of the mean
TBARs = thiobarbituric acid reactants
Tfam = mitochondrial transcription factor A
TLR4 = Toll-like receptor 4
TNF-α = tumor necrosis factor-alpha
WT = wild type

This article has been cited by:

1. Antero Salminen, Johanna Ojala, Kai Kaarniranta, Anu Kauppinen. 2012. Mitochondrial dysfunction and oxidative stress activate inflammasomes: impact on the aging process and age-related diseases. *Cellular and Molecular Life Sciences* **69**:18, 2999-3013. [CrossRef]
2. Claude A. Piantadosi, Hagir B. Suliman. 2012. Redox regulation of mitochondrial biogenesis. *Free Radical Biology and Medicine* . [CrossRef]
3. Claude A. Piantadosi, Hagir B. Suliman. 2012. Transcriptional control of mitochondrial biogenesis and its interface with inflammatory processes. *Biochimica et Biophysica Acta (BBA) - General Subjects* **1820**:4, 532-541. [CrossRef]